[redacted]

Copy
RM L54A15

NACA RM L54A15

RESEARCH MEMORANDUM

TRANSONIC WIND-TUNNEL INVESTIGATION OF THE EFFECTS OF TAPER RATIO, BODY INDENTATION, FIXED TRANSITION, AND AFTERBODY SHAPE ON THE AERODYNAMIC CHARACTERISTICS OF A 45° SWEPTBACK WING-BODY COMBINATION

By Francis G. Morgan, Jr. and Melvin M. Carmel

Langley Aeronautical Laboratory
Langley Field, Va.

CLASSIFICATION CHANGED
UNCLASSIFIED

To ________________________________

NACA Res abs effective
By authority of + RN-121 Date Oct 14, 1957
Amt 11-15-57

CLASSIFIED DOCUMENT

This material contains information affecting the National Defense of the United States within the meaning of the espionage laws, Title 18, U.S.C., Secs. 793 and 794, the transmission or revelation of which in any manner to an unauthorized person is prohibited by law.

NATIONAL ADVISORY COMMITTEE
FOR AERONAUTICS

WASHINGTON
March 15, 1954

[redacted]

1X

NATIONAL ADVISORY COMMITTEE FOR AERONAUTICS

RESEARCH MEMORANDUM

TRANSONIC WIND-TUNNEL INVESTIGATION OF THE EFFECTS OF TAPER RATIO, BODY INDENTATION, FIXED TRANSITION, AND AFTERBODY SHAPE ON THE AERODYNAMIC CHARACTERISTICS OF A 45° SWEPTBACK WING-BODY COMBINATION

By Francis G. Morgan, Jr. and Melvin M. Carmel

SUMMARY

An investigation has been made to determine the effects of taper ratio, body indentation, fixed transition, and afterbody shape on the transonic aerodynamic characteristics of a 45° sweptback wing-body combination having an aspect ratio of 4. The results were obtained in the Langley 8-foot transonic tunnel at Mach numbers from 0.80 to 1.15, angles of attack from 0° to 12°, and Reynolds numbers varying from 1.80×10^6 to 2.00×10^6 based on the mean aerodynamic chord of the wings.

The results show that the low-taper-ratio wing has the greater drag coefficients at zero lift above a Mach number of 0.93 and also the higher incremental zero-lift drag-rise coefficients. Body indentation, however, essentially eliminates these adverse effects of lower taper ratio. Furthermore, at a Mach number of 1.00, body indentation leads to an increase in maximum lift-drag ratio of 40 percent for the low-taper-ratio wing and an increase of 30 percent for the higher-taper-ratio wing. Although the data are not conclusive, it is possible that there is little effect from increasing the region of turbulent flow on the effect of indentation on the zero-lift drag-rise coefficients. The boattailed body has greater wing-body interference than does the wing-body combination with the cylindrical body. However, body indentation reduces this difference in wing-body interference between the two bodies. No appreciable changes in pitch-up occur with the use of body indentation.

[redacted]

INTRODUCTION

Designers of transonic and low supersonic speed aircraft are currently showing interest in the performance of low-taper-ratio wings because of the increased strength derived from lowering the taper ratio while keeping the other wing variables constant. At the present time, little data are available on the effect of such reductions in taper ratio on the aerodynamic characteristics of wing-body combinations in the transonic speed range. Since the transonic drag-rise rule of reference 1 shows that body indentation effects a reduction in drag rise at zero lift for wing-body combinations near the speed of sound, it was deemed advisable to determine the effect of body indentation on models with different taper ratio.

Up to the present time, nearly all investigations of indentation have been made with wing-body configurations on which extensive regions of laminar flow have been present. Since the end result of body indentation is for use on full-scale aircraft, it is important to ascertain the effectiveness of body indentation for a condition for which the flow is primarily turbulent. An attempt was made to ascertain the effect of this predominantly turbulent flow.

With these problems in mind, the subject investigation was initiated in the Langley 8-foot transonic tunnel. In addition, the test program supplied information on the effects of changing afterbody shape. The results were obtained at Mach numbers from 0.80 to 1.15, angles of attack from 0° to 12°, and Reynolds numbers from 1.80×10^6 to 2.00×10^6 based on the mean aerodynamic chord of the wings.

SYMBOLS

$\bar{c}$	mean aerodynamic chord
C_D	drag coefficient
C_{D_O}	zero-lift drag coefficient
ΔC_{D_O}	zero-lift drag-rise coefficient
$C_{D_{C_L=0.3}} - C_{D_{C_L=0}}$	incremental drag coefficient between lift coefficients of 0 and 0.3
C_L	lift coefficient

C_{L_α} slope of the lift curve between $C_L = 0$ and $C_L = 0.2$

$C_{L_{pitch\text{-}up}}$ lift coefficient at which pitch-up occurs

C_m pitching-moment coefficient about the 0.25-chord point of $\bar{c}$

$C_{m_{C_L}}$ slope of pitching-moment curve between $C_L = 0$ and $C_L = 0.2$

D drag, lb

L lift, lb

$(L/D)_{max}$ maximum lift-drag ratio

M Mach number

α angle of attack, deg

λ taper ratio

p_b base static pressure

p_o free-stream static pressure

q free-stream dynamic pressure

P_b base pressure coefficient, $\frac{p_b - p_o}{q}$

APPARATUS AND METHODS

Tunnel

The subject tests were conducted in the Langley 8-foot transonic tunnel which is a dodecagonal, single-return, slotted wind tunnel designed to obtain aerodynamic data through the speed of sound without the usual choking and blockage effects associated with a conventional closed-throat type of wind tunnel. The tunnel operates at atmospheric stagnation pressures. A more detailed description of this tunnel may be found in reference 2.

Configurations

The low-taper-ratio wing tested has 45° sweepback of the 0.25-chord line, an aspect ratio of 4, a taper ratio of 0.3, and NACA 65A006 airfoil sections parallel to the model plane of symmetry. This wing is of solid aluminum-alloy construction and is similar to that used in reference 3. The other wing tested has the same geometric characteristics as the first wing except that the taper ratio is 0.6. It is of solid steel construction. Both wings were tested as midwing configurations. The body was originally the cylindrical body of reference 4. This body was modified in such a way that the cylindrical portion extended rearward only 4 inches from the forebody and the afterbody was boattailed to an overall body length of 41.25 inches. Dimensional details for the wing-body combinations tested may be found in figure 1.

The outer portion of the body was made of detachable, wood-impregnated plastic between stations 22.5 and 36.9 inches aft of the model nose. In order to ascertain the effects of body indentation on wing-body combinations with varied wing taper ratios, an additional body was made for each wing in a manner such that the axial cross-sectional area development of each wing-body combination was the same as that for the basic body alone. Still another body was tested consisting of the basic body with a symmetrical bump simulating the axial cross-sectional area development of the low-aspect-ratio-wing—body combination. Ordinates for these test bodies may be found in table I, and the axial cross-sectional area developments for all test configurations may be found in figure 2.

In order to investigate the effect of fixed transition, 1/8-inch carborundum strips were placed at 10 percent of the wing chord (upper and lower surface) and around the periphery of the body at a position 1/4 inch forward of the maximum diameter. However, these strips were blown off of the basic configuration during the testing, and a repeat run was unavailable.

The model was attached to the forward end of an internal electrical strain-gage balance. This balance was attached, by means of a sting, to the tunnel central support system.

Measurements and Accuracy

The average free-stream Mach number was determined to within ±0.003 from a calibration with respect to the pressure in the chamber surrounding the slotted test section.

The accuracy of the lift, drag, and pitching-moment coefficients, based on calibration and the reproducibility of the data, is believed to be within ±0.01, ±0.001, and ±0.002, respectively.

The drag data have been adjusted for base pressure such that the drag corresponds to conditions for which the body base pressure would be equal to the free-stream static pressure.

No basic data were obtained between Mach numbers of 1.03 and 1.15 because of tunnel-wall shock-reflection effects (ref. 5). Unpresented schlieren data from the present test indicate that there would be little effect of tunnel-wall shock reflection on the drag data at $M = 1.15$. On all cross-plotted data, however, the data between $M = 1.03$ and $M = 1.15$ were connected with an arbitrary fairing.

The angle of attack of the model was measured by a pendulum-type accelerometer mounted in the model nose. This instrument, at a relatively constant temperature, measured angles within $\pm 0.02^{\circ}$. Because of the large temperature changes that occur during tests throughout the Mach number range, however, the zero of the instrument varied. Therefore, the readings of this instrument were checked at an angle of attack of 0° by a selsyn unit, which is insensitive to temperature variation, installed at the pivot point of the mechanism that changed the angle of attack. The accuracy of this device at this condition was ± 0.05. The overall accuracy was $\pm 0.10^{\circ}$.

PRESENTATION OF RESULTS

The variation of angle of attack, drag coefficient, and pitching-moment coefficient with lift coefficient for all of the wing-body configurations of the subject investigation are presented in figures 3 to 5. The corresponding base pressure coefficients for the subject investigation may be found in figure 6. The variations of drag, incremental drag-rise coefficient, drag due to lift, and maximum lift-drag ratio with Mach number are found in figures 7 to 17. The body used to simulate the axial cross-sectional area of the low-taper-ratio-wing—body configuration and the basic body alone were tested only at zero-lift conditions, as shown in figures 7 and 11. The variation of lift-curve slope, pitching-moment-curve slope, and lift coefficient for pitch-up with Mach number are shown in figures 18 and 19.

In order to facilitate presentation of the data, staggered scales have been used in many figures, and, therefore, care should be taken in identifying the zero axis for each curve.

Reference to wings in this discussion refers to data presented for wing-body configurations.

DISCUSSION

Drag Characteristics

Taper-ratio effects.- The variations of drag coefficient with Mach number for the two wings tested on the basic body are shown in figure 7. In the Mach number range below 0.93, the zero-lift drag-coefficient values are the same for both the low-taper-ratio wing and the higher-taper-ratio wing. These values are approximately the same as those presented in reference 3 for similar wings on a different body. The slight differences which do exist are within the experimental accuracy of the two sets of data. Figure 7 also shows that the drag coefficients, for the 0.3 lift condition, are slightly higher throughout the Mach number range for the low-taper-ratio wing. Above a Mach number of 0.96, this difference is approximately the same as that for the zero-lift condition.

Figure 8 shows that the low-taper-ratio wing has higher incremental drag-rise coefficient values above a Mach number of 0.93 than does the higher-taper-ratio wing. At a Mach number of 1.00, the drag-rise value for the low-taper-ratio wing is 32 percent higher than for the higher-taper-ratio wing. This increase is in qualitative agreement with the transonic drag-rise rule (ref. 1) since, as is shown in figure 2, the low-taper-ratio wing has both the greater maximum area and the more abrupt cross-sectional area development.

Up to a Mach number of 1.00 the low-taper-ratio wing has higher incremental drag coefficients due to lift than does the higher-taper-ratio wing (fig. 9). Above a Mach number of 1.00, the higher-taper-ratio wing has the higher incremental drag coefficients. These differences, however, are generally within the experimental accuracies of these data.

The maximum lift-drag ratios (fig. 10) for the low-taper-ratio wing are lower throughout the test Mach number range than those for the higher-taper-ratio wing.

In order to determine whether the transonic drag-rise rule is effective in correlating the drag rise of the low-taper-ratio wing, a body of revolution with the same axial cross-sectional area distribution as the low-taper-ratio-wing—body configuration was tested. The drag-rise coefficient was less throughout the transonic speed range for the equivalent body (fig. 11). At a Mach number of 1.00 the value was 35 percent lower. This value of 35 percent at $M = 1.00$ compares favorably with the percentage difference between the higher-taper-ratio-wing—body combination and its equivalent body of reference 1.

Influence of body indentation.- From figures 12 and 13, it may be seen that indenting the body for the low-taper-ratio wing reduces the drag coefficient and incremental drag-rise coefficient values more in the transonic speed range than a similar indentation for the higher-taper-ratio wing. The drag-rise coefficients for the two indented configurations are approximately the same within the limits of experimental accuracy throughout the entire test Mach number range. Thus, the adverse effect on the zero-lift drag rise of lowering the taper ratio is essentially eliminated by body indentation.

Figure 14 shows that body indentation has little effect on the incremental drag coefficient due to lift between lift coefficients of 0 and 0.3 for either the low-taper-ratio or high-taper-ratio wings except in the critical Mach number range around 0.96, where the incremental drag coefficient amounts to 0.004 for the low-taper-ratio wing and 0.003 for the higher-taper-ratio wing. Figure 15 shows that maximum lift-drag ratios are increased for both wings by indentation. At a Mach number of 1.00, body indentation leads to an increase in maximum lift-drag ratio of 40 percent for the low-taper-ratio wing and an increase of 30 percent for the higher-taper-ratio wing.

Effect of transition on drag rise.- Nearly all of the investigations of the transonic drag-rise rule have been made with wing-body configurations for which extensive regions of laminar flow were prevalent. One of the questions arising from this type of investigation concerns the effectiveness of body indentation when there are extensive regions of turbulent flow present. (Such flow is generally found on full-scale aircraft.) The incremental drag-rise coefficient results for the indented wing-body configuration with fixed transition are shown in figure 16, compared with results for the same wing-body configuration without fixed transition. A comparison of the results tends to show that fixing transition in the manner employed herein did not affect the drag-rise coefficient values up to a Mach number of 1.00, and at Mach numbers of 1.03 and 1.15 the effects were small.

Two tests were made with the low-taper-ratio wing on the basic body with both configurations having the same visible surface conditions. However, there was a drag-coefficient differential between the two tests of 0.0025 at subsonic Mach numbers. Unpublished data from the Langley low turbulence pressure tunnel for this same model show a similar drag differential caused by fixing the transition at the same chordwise position as was used on the indented wing-body configuration of this test. It is therefore possible that the additional drag for one of the basic configurations tested in the 8-foot transonic tunnel was due to some surface condition which caused transition to move forward on the wing. If this assumption is true, the comparison of the incremental drag-rise coefficients (fig. 16) tends to indicate that there are no effects of transition on the drag-rise coefficient values of the basic configuration. This also leads to the possible assumption that transition has little effect on the effectiveness of body indentation on the zero-lift drag-rise coefficient values.

Effect of afterbody shape.- Tests of the effects of body indentation with the higher-taper-ratio wing have previously been made with a body that differed from the present body in that it had a cylindrical afterbody (ref. 4). This type of body was previously used in order to reduce adverse wing-body interference, and also to reduce the effects of tunnel-wall shock reflection on the drag at zero lift for the maximum obtainable Mach number. The boattailed afterbody, however, is more nearly like the bodies being used on present-day operational aircraft. Therefore, it is believed desirable to present a comparison of the effects of body indentation on wing-body interference for the two basic body shapes. The drag-coefficient curves on figure 17 are for the wing-body configuration drag coefficients minus the basic body alone drag coefficients. It must be pointed out that these data may not be exactly comparable due to possible small sting interference on the wing and the effect of the wing on the base pressure. It is felt, however, that some idea of the relative merits of the two afterbody shapes may be obtained.

A comparison of the curves on figure 17 shows that the drag values for the wing plus wing-body interference of the boattailed configuration at Mach numbers above 0.95 are greater than those for the cylindrical body of reference 1. At a Mach number of 1.00, the drag coefficients for the two basic configurations differ by 0.0048. It may also be seen from figure 17 that body indentation considerably reduces the wing-body interference in the transonic speed range. At subsonic Mach numbers, the differences in wing-body interference, for the two wings with and without indentation, are approximately the same within experimental accuracies.

Lift and Stability Characteristics

The slope of the lift curve (fig. 18) is less throughout the entire Mach number range for the low-taper-ratio wing than for the higher-taper-ratio wing on the basic body. When the bodies were indented, both wings had essentially the same lift-curve slope except in the Mach number range from about 0.90 to 1.00. In this range the low-taper-ratio wing has the higher values.

The variation of pitching-moment-curve slope with Mach number (fig. 18) is approximately the same for both basic configurations, although the low-taper-ratio wing is more stable throughout the entire test Mach number range. The trend of the results shows that body indentation decreases the longitudinal stability of the low-taper-ratio wing up to a Mach number of 1.10 and up to a Mach number of 1.06 for the higher-taper-ratio wing. Above these Mach numbers body indentation effects increases in longitudinal stability. Figure 19 shows that, at subsonic speeds, the lift coefficient at which pitch-up occurs is approximately 0.1 lower for the low-taper-ratio wing than for the higher-taper-ratio wing. The trend of the basic data shows that above a Mach number of 1.00, the lift coefficient at which pitch-up occurs for the low-taper-ratio wing approaches that for the higher-taper-ratio wing. No appreciable changes in pitch-up characteristics occurred with the use of body indentation.

CONCLUDING REMARKS

A transonic wind-tunnel investigation of the effects of taper-ratio variation on the aerodynamic characteristics of a 45° sweptback wing-body combination shows that the low-taper-ratio wing has the greater drag coefficients at zero lift above a Mach number of 0.93 and also the higher incremental zero-lift drag-rise coefficients. Upon indenting the bodies, the adverse effect on drag coefficient and incremental drag rise, caused by lowering the taper ratio, is essentially eliminated. Furthermore, at a Mach number of 1.00, body indentation leads to an increase in maximum lift-drag ratios of 40 percent for the low-taper-ratio wing and an increase of 30 percent for the higher-taper-ratio wing. Although the data are not conclusive, it is possible that there is little effect from increasing the region of turbulent flow on the effect of indentation on the zero-lift drag-rise coefficients.

A configuration with a boattailed body has greater wing-body interference drag than the same configuration with a cylindrical body. However, body indentation considerably reduces this difference in wing-body interference between the boattailed and cylindrical bodies in the transonic speed range.

No appreciable changes in pitch-up occur with the use of body indentation.

Langley Aeronautical Laboratory,
National Advisory Committee for Aeronautics,
Langley Field, Va., January 5, 1954.

REFERENCES

1. Whitcomb, Richard T.: A Study of the Zero-Lift Drag-Rise Characteristics of Wing-Body Combinations Near the Speed of Sound. NACA RM L52H08, 1952.

2. Wright, Ray H., and Ritchie, Virgil S.: Characteristics of a Transonic Test Section With Various Slot Shapes in the Langley 8-Foot High-Speed Tunnel. NACA RM L51H10, 1951.

3. King, Thomas J., Jr., and Pasteur, Thomas B., Jr.: Wind-Tunnel Investigation of the Aerodynamic Characteristics in Pitch of Wing-Fuselage Combinations at High Subsonic Speeds - Taper-Ratio Series. NACA RM L53E20, 1953.

4. Robinson, Harold L.: A Transonic Wind-Tunnel Investigation of the Effects of Body Indentation, As Specified by the Transonic Drag-Rise Rule, on the Aerodynamic Characteristics and Flow Phenomena of a 45° Sweptback-Wing—Body Combination. NACA RM L52L12, 1953.

5. Ritchie, Virgil S., and Pearson, Albin O.: Calibration of the Slotted Test Section of the Langley 8-Foot Transonic Tunnel and Preliminary Experimental Investigation of Boundary-Reflected Disturbances. NACA RM L51K14, 1952.

TABLE I.- BODY COORDINATES

Forebody		Afterbody							
		Basic body		Indented body with wing of 0.6 taper ratio		Indented body with wing of 0.3 taper ratio		Equivalent body for the wing-body combination with wing of 0.3 taper ratio	
Station, in. from nose	Radius, in.	Station, in. from nose	Radius, in.	Station, in. from nose	Radius, in.	Station, in. from nose	Radius, in.	Station, in. from nose	Radius, in.
0	0	22.500	1.875	22.500	1.875	22.500	1.875	22.5	1.875
.225	.104	26.500	1.875	23.100	1.875	23.380	1.875	23.380	1.875
.5625	.193	27.692	1.868	23.625	1.864	23.692	1.863	23.692	1.883
1.125	.325	28.692	1.862	24.625	1.812	24.692	1.819	24.692	1.924
2.250	.542	29.692	1.849	25.625	1.742	25.692	1.749	25.692	1.984
3.375	.726	30.692	1.825	26.625	1.650	26.692	1.662	26.692	2.045
4.500	.887	31.692	1.789	27.625	1.595	27.692	1.579	27.692	2.096
6.750	1.167	32.692	1.745	28.625	1.551	28.692	1.505	28.692	2.140
9.000	1.390	33.692	1.694	29.625	1.537	29.692	1.468	29.692	2.149
11.250	1.559	34.692	1.638	30.625	1.537	30.692	1.469	30.692	2.118
13.500	1.683	35.692	1.570	31.625	1.530	31.692	1.490	31.692	2.042
15.750	1.770	36.692	1.486	32.625	1.499	32.692	1.505	32.692	1.957
18.000	1.828	36.900	1.468	33.625	1.472	33.692	1.506	33.692	1.861
20.250	1.864	37.500	1.408	34.625	1.468	34.692	1.502	34.692	1.762
		38.500	1.298	35.625	1.468	35.692	1.491	35.692	1.649
		39.500	1.167	36.625	1.468	36.692	1.471	36.692	1.508
		40.500	1.030	36.900	1.468	36.900	1.468	36.900	1.468
		41.250	.937						

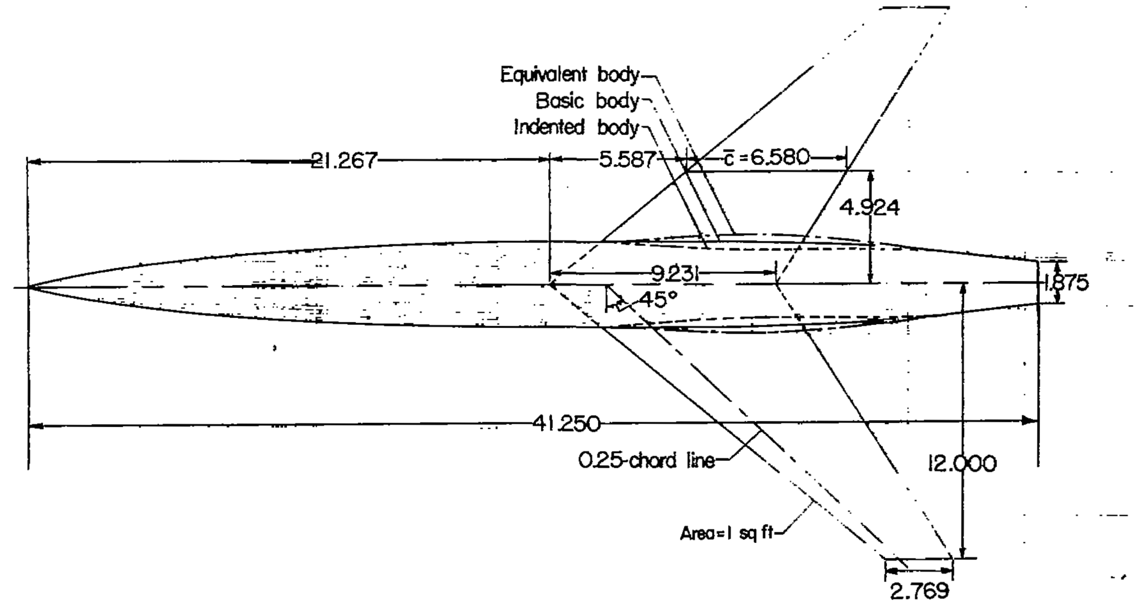

(a) Wing-body configuration with taper ratio of 0.3.

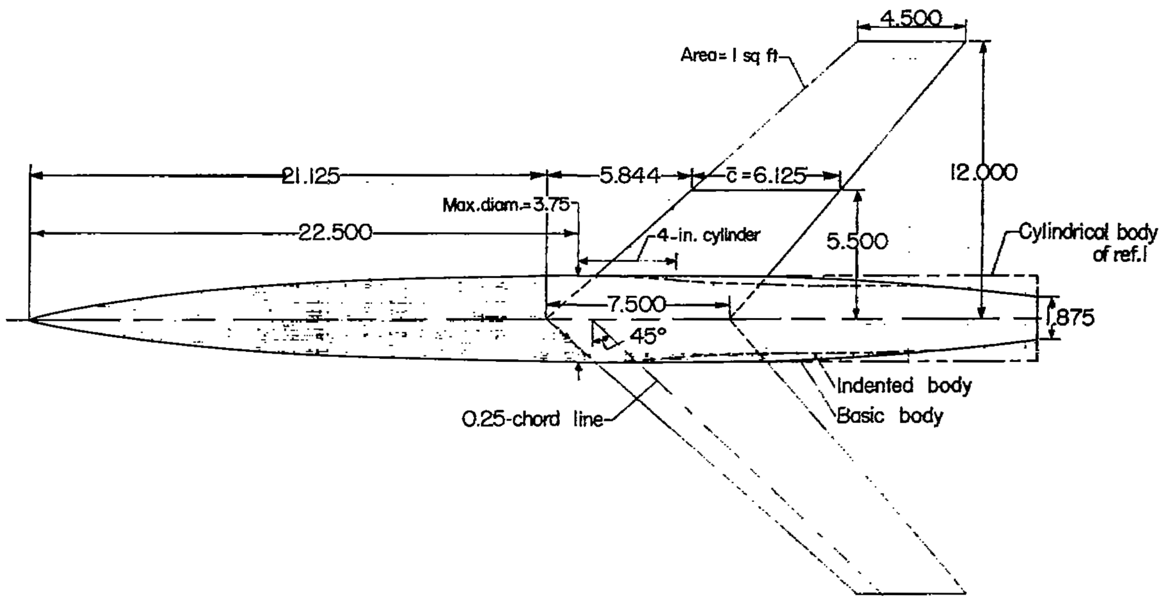

(b) Wing-body configuration with taper ratio of 0.6.

Figure 1.- Wing-body configurations used in investigation. All dimensions are in inches.

[redacted]

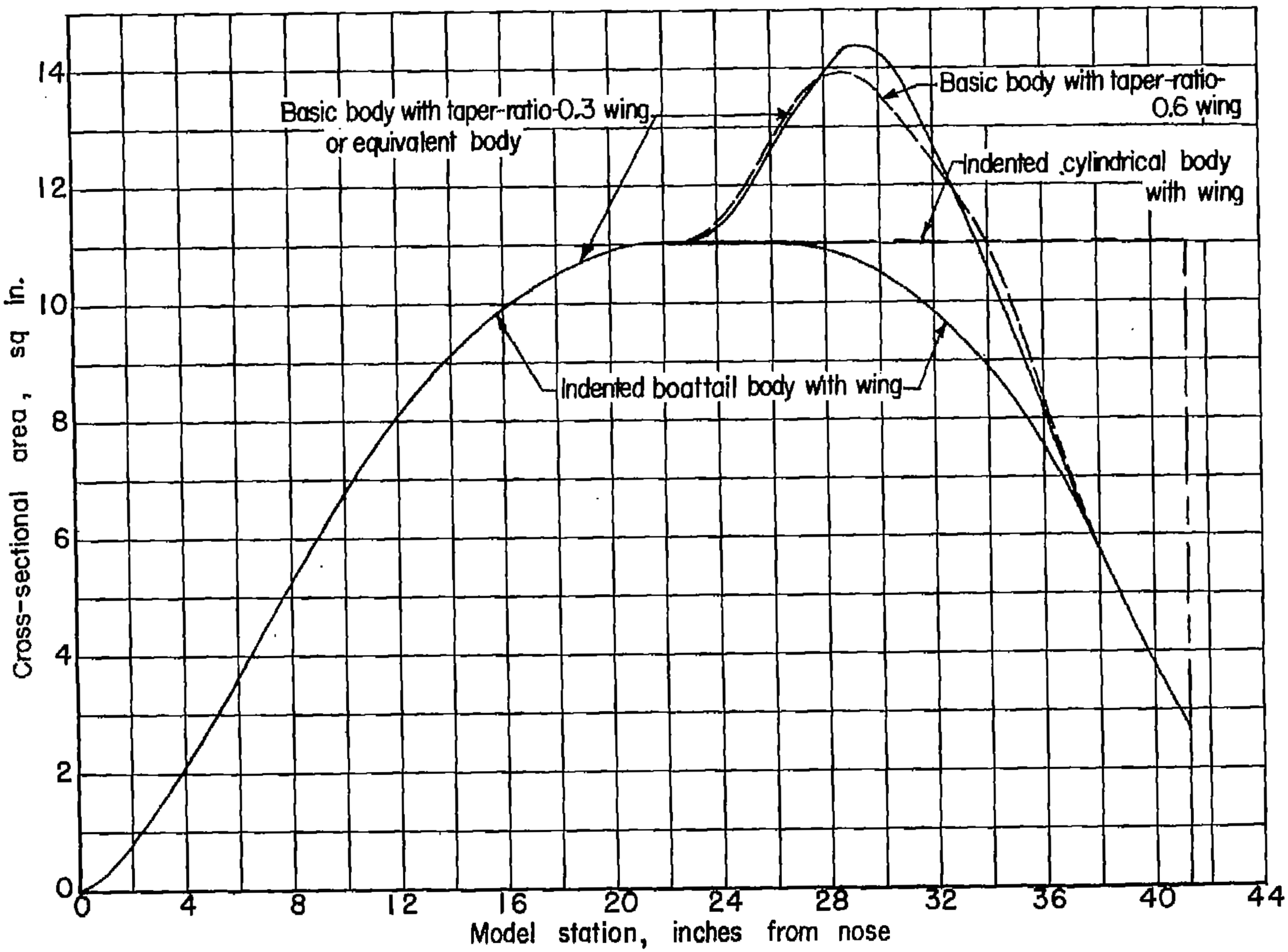

Figure 2.- Axial cross-sectional area development of wing-body configurations tested.

[redacted]

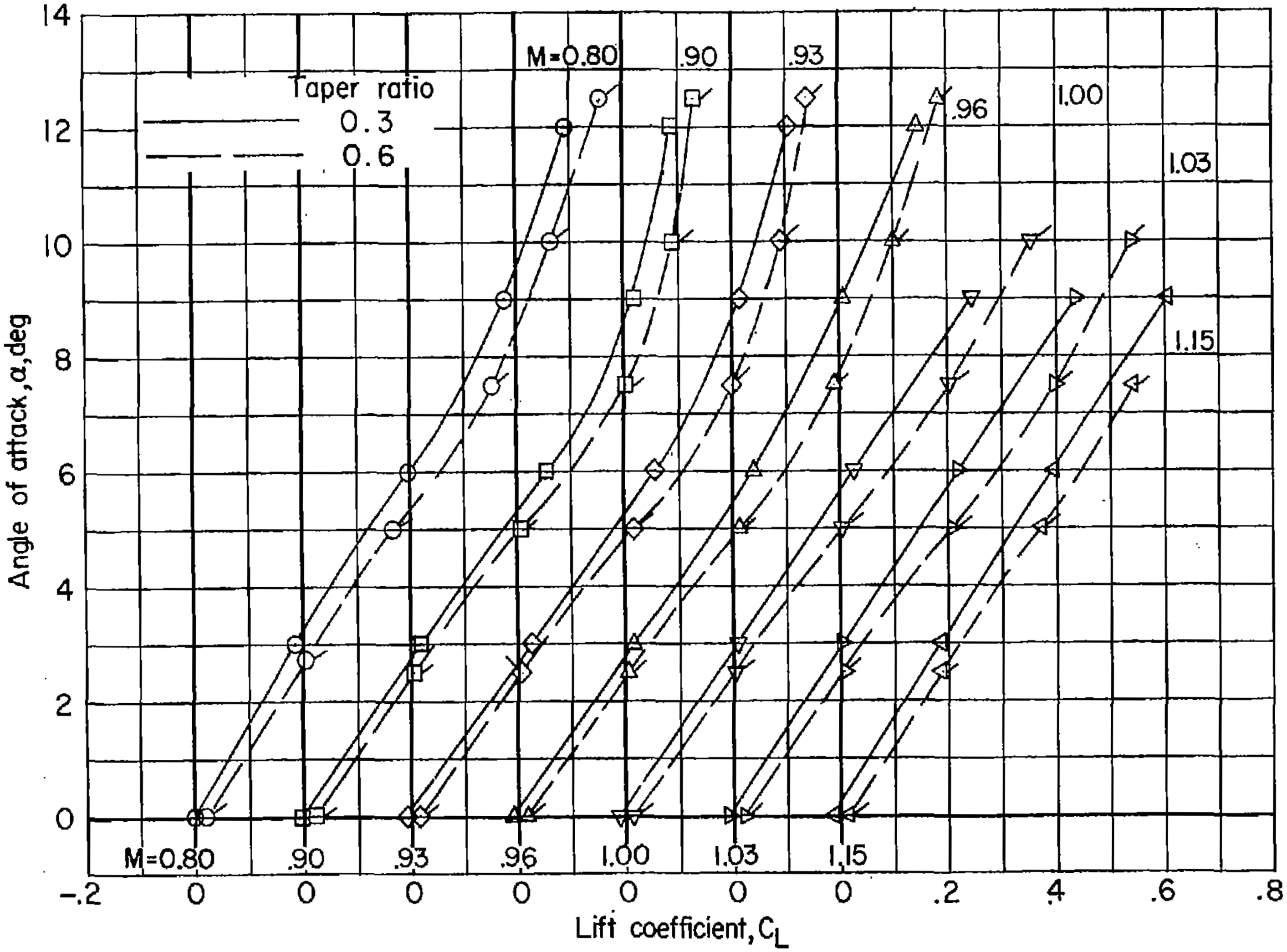

(a) Angle of attack.

Figure 3.- Aerodynamic characteristics of the basic wing-body combinations.

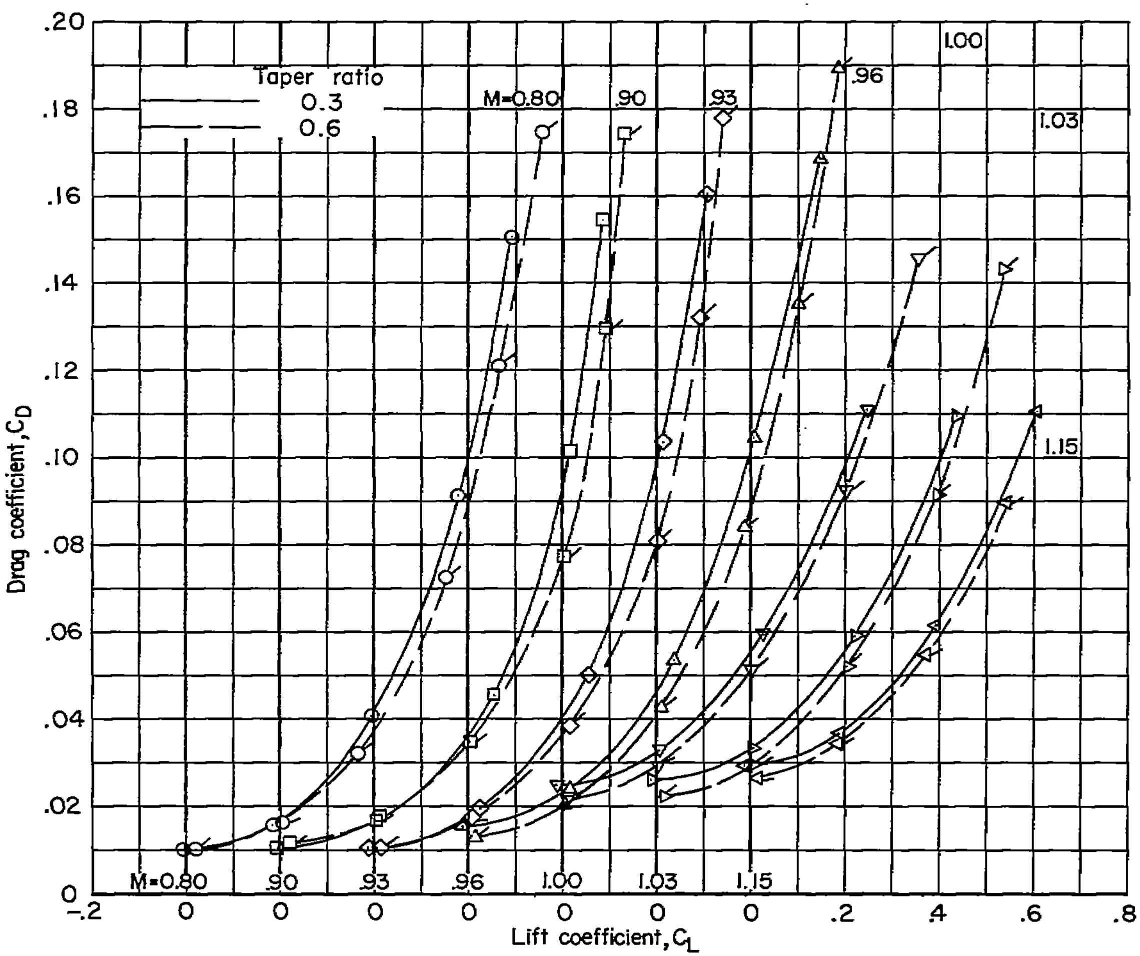

(b) Drag coefficient.

Figure 3.- Continued.

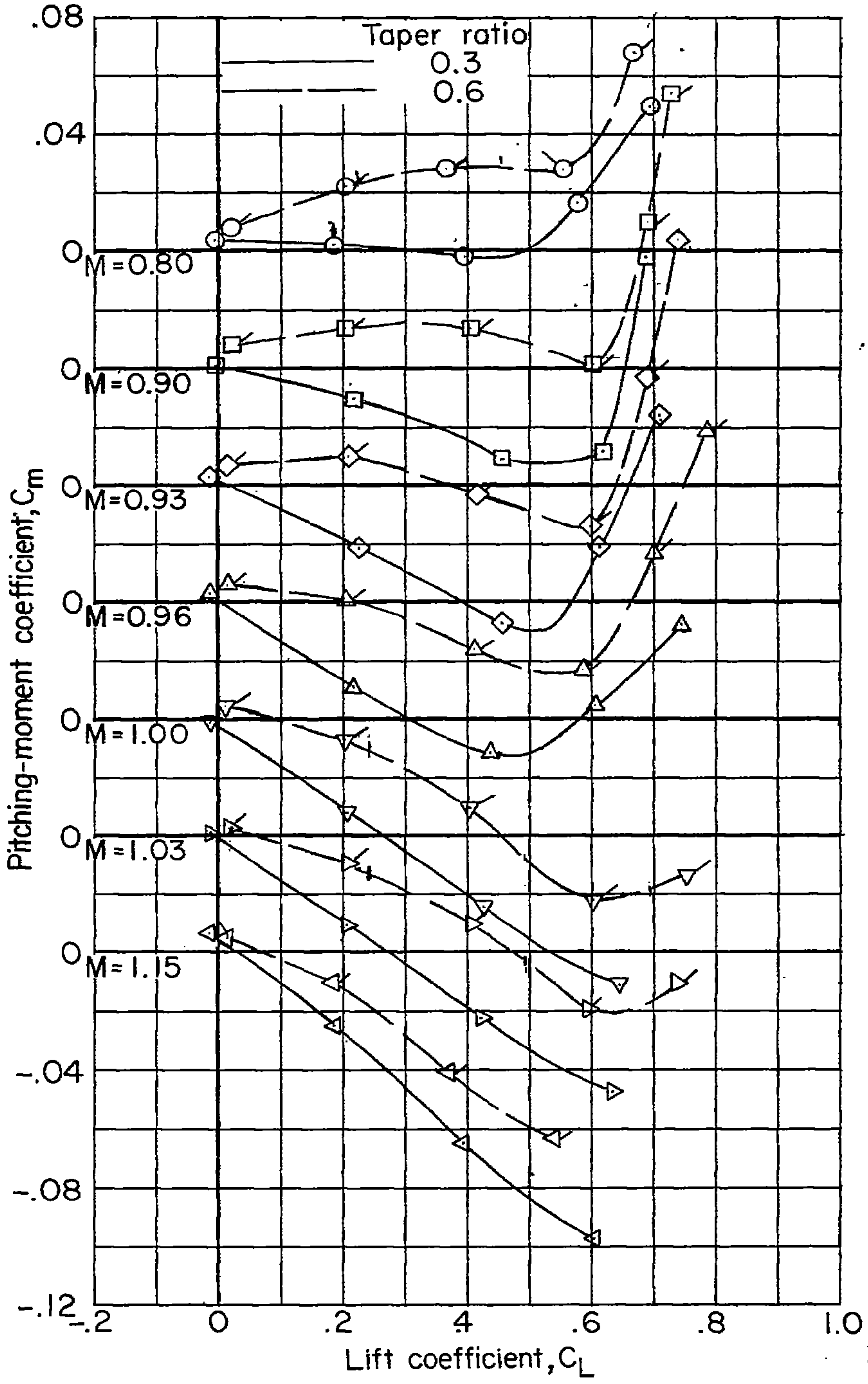

(c) Pitching-moment coefficient.

Figure 3.- Concluded.

[redacted]

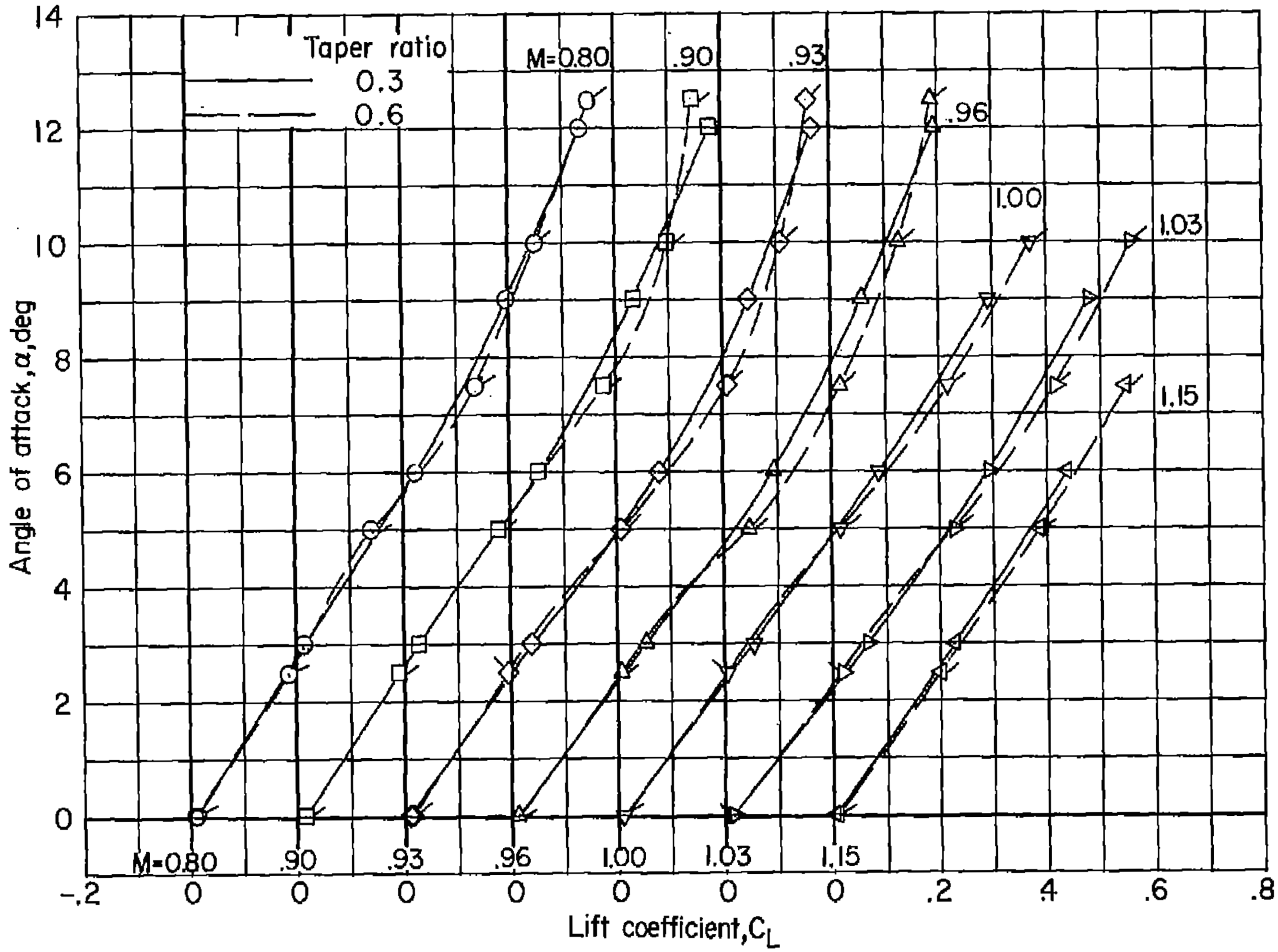

(a) Angle of attack.

Figure 4.- Aerodynamic characteristics of the indented wing-body combinations.

[redacted]

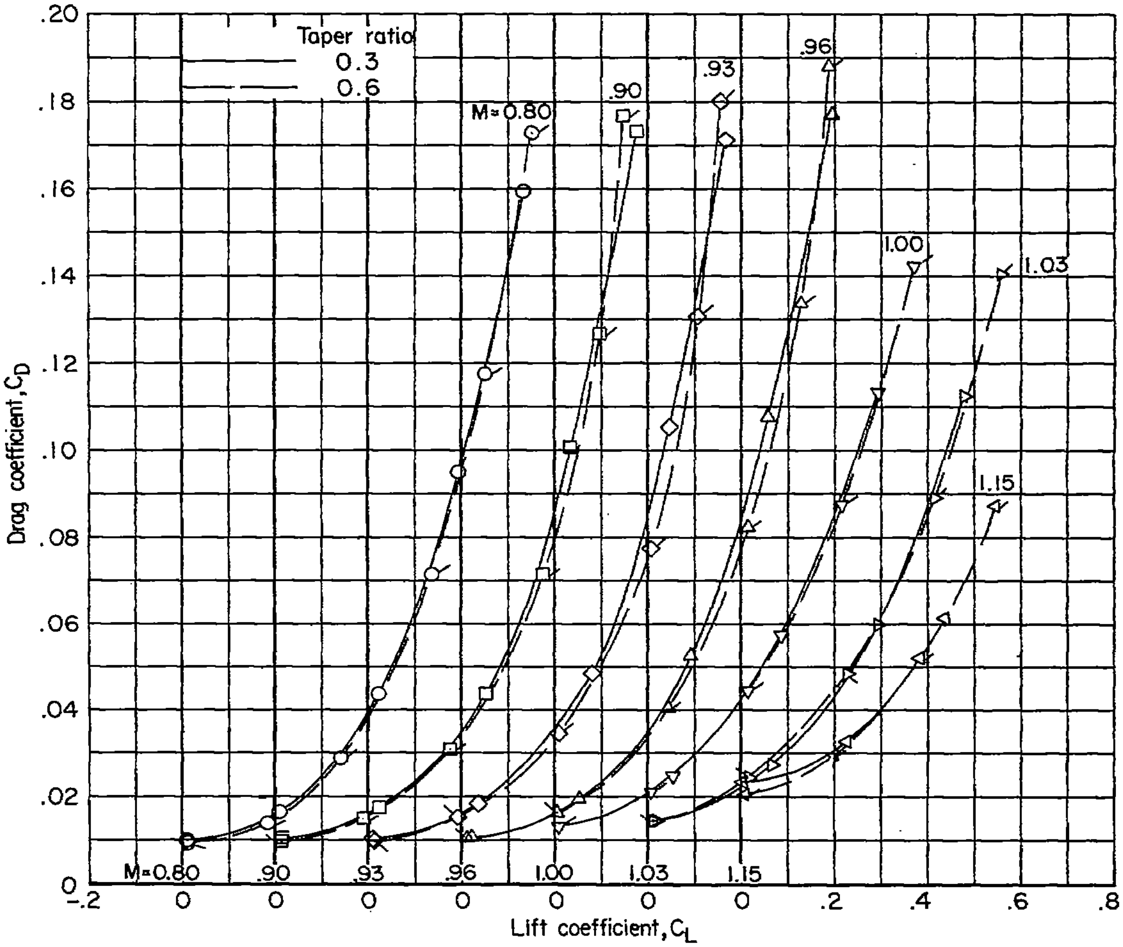

(b) Drag coefficient.

Figure 4.- Continued.

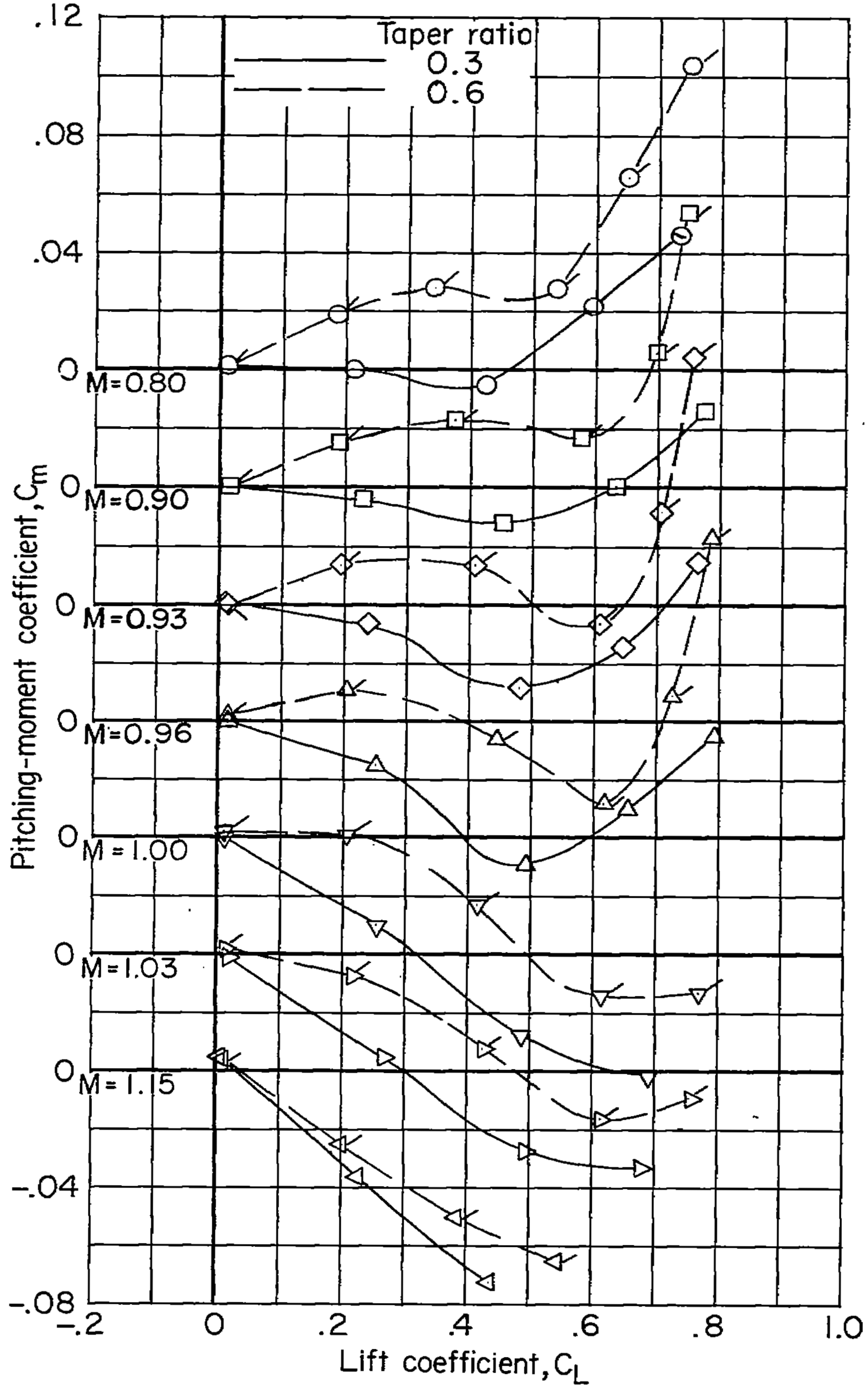

(c) Pitching-moment coefficient.

Figure 4.- Concluded.

[redacted]

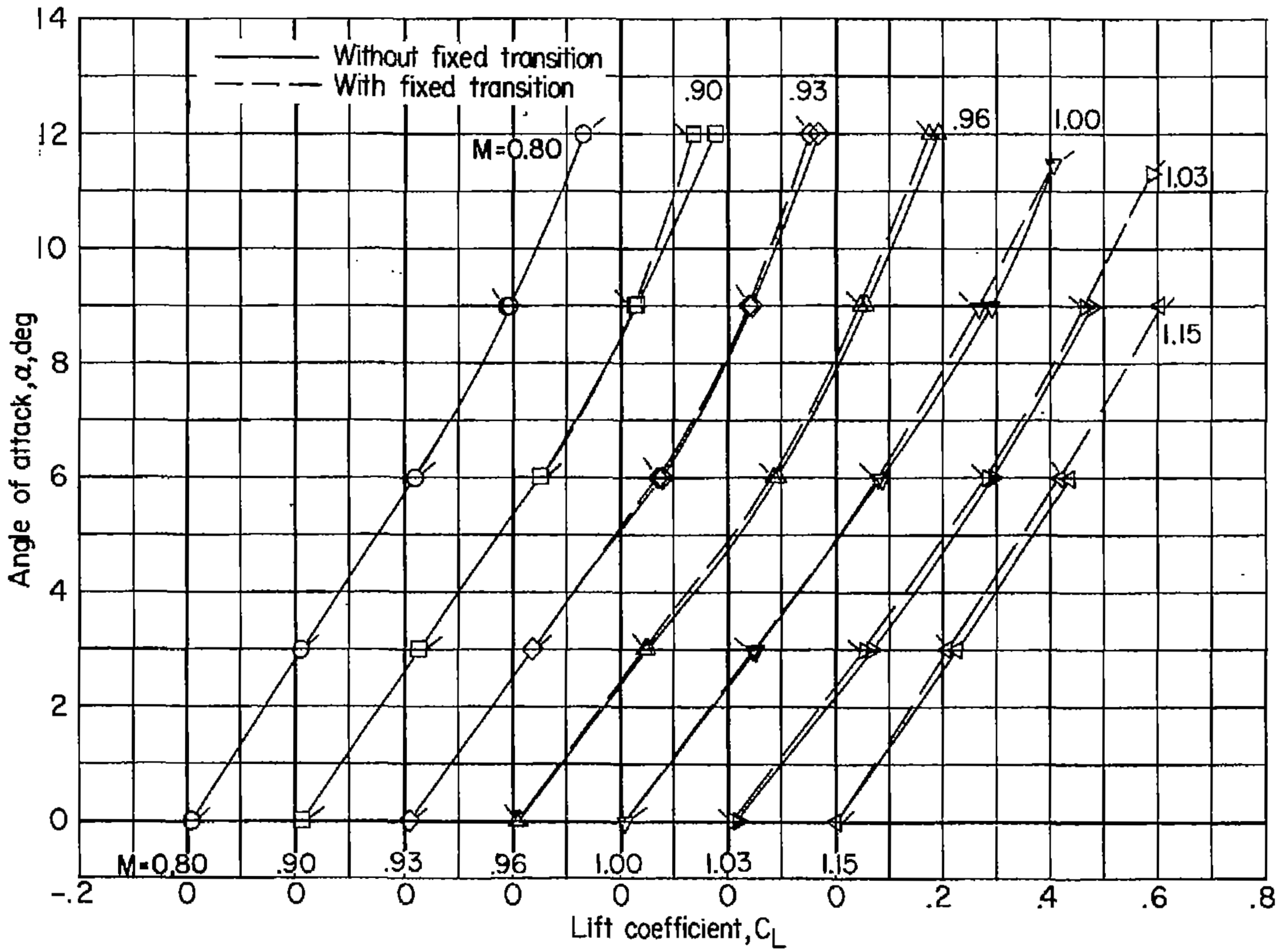

(a) Angle of attack.

Figure 5.- Aerodynamic characteristics of the low-taper-ratio-wing—body combination with and without fixed transition.

[redacted]

[redacted]

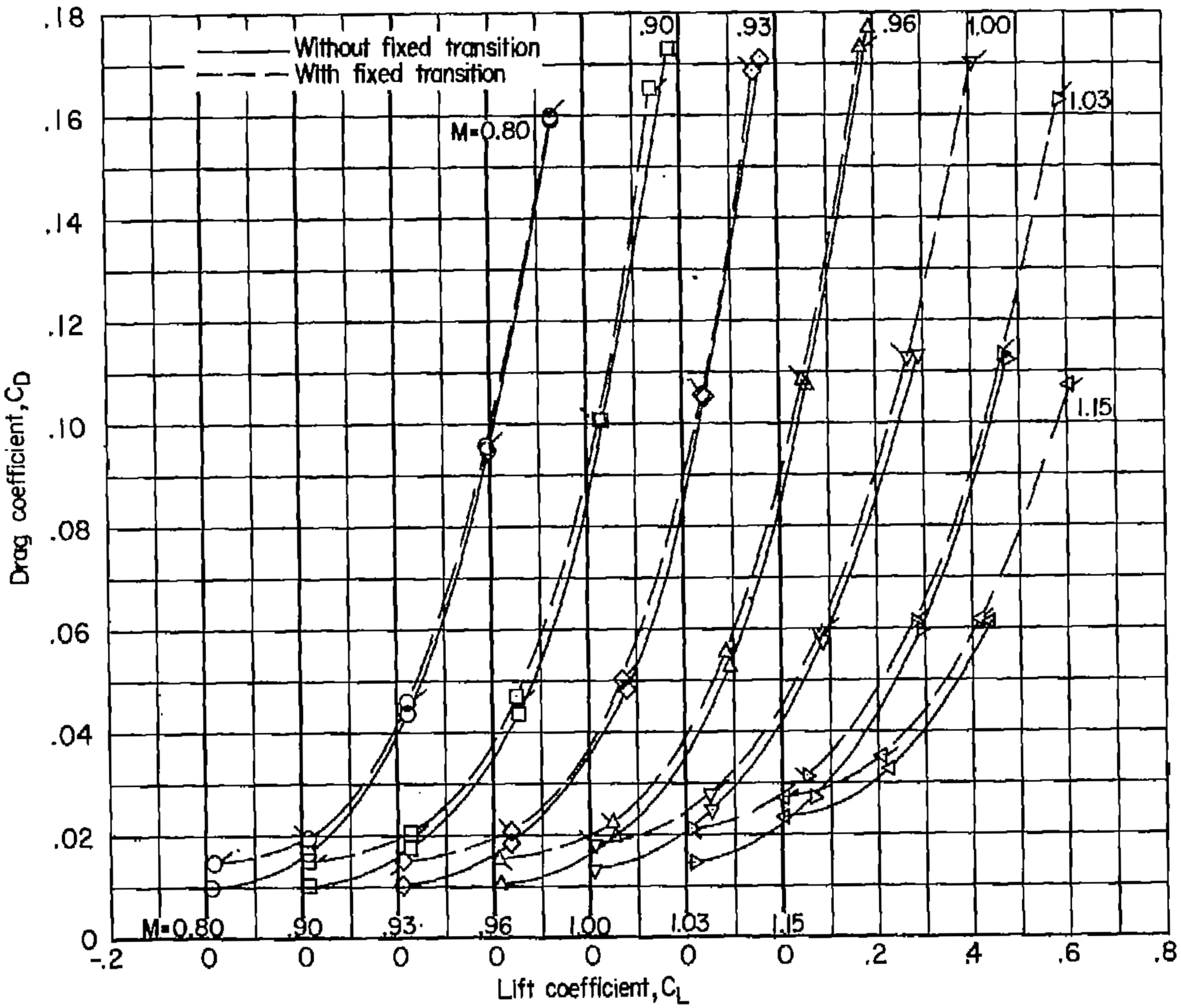

(b) Drag coefficient.

Figure 5.- Continued.

[redacted]

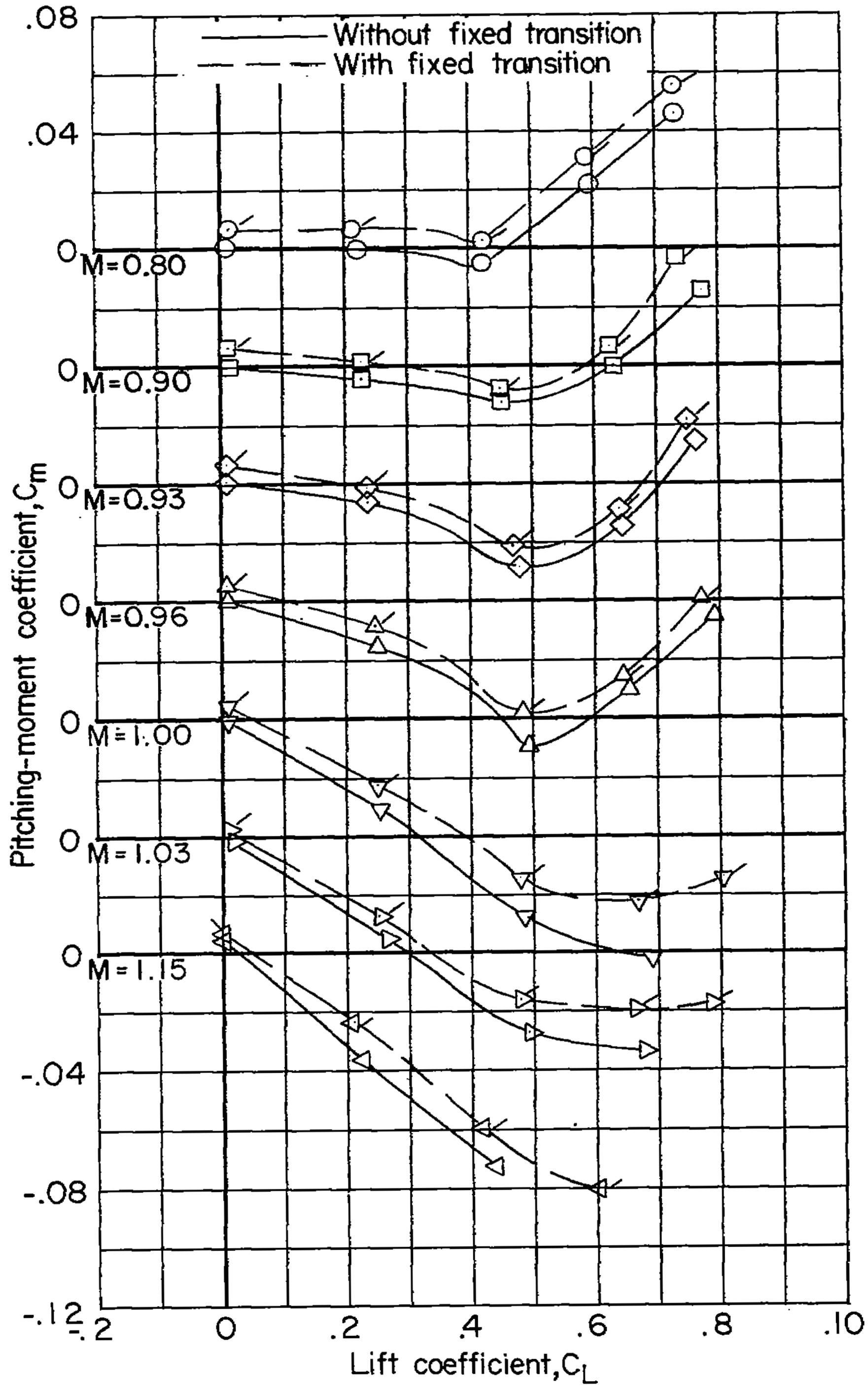

(c) Pitching-moment coefficient.

Figure 5.- Concluded.

[redacted]

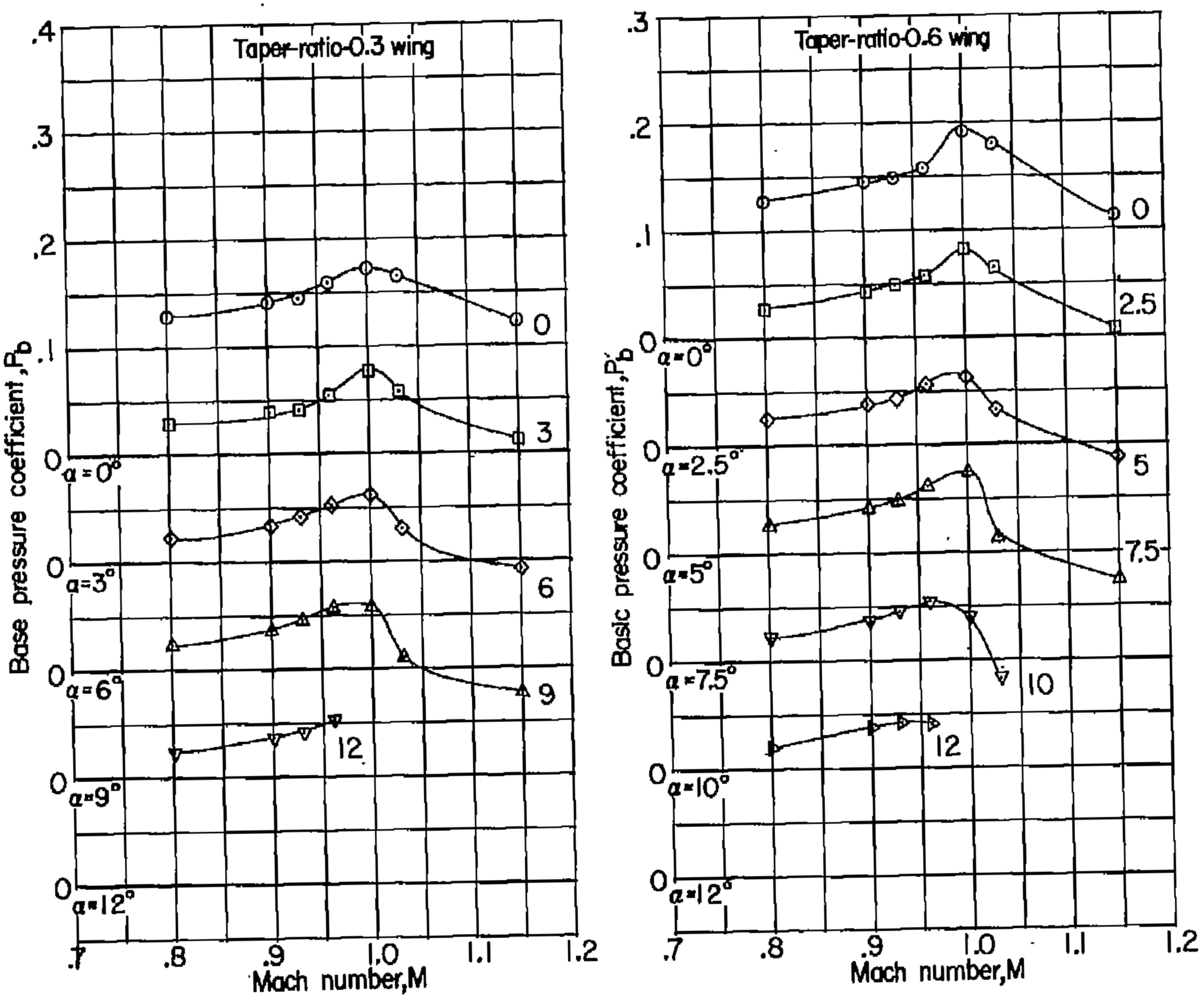

(a) Basic body.

Figure 6.- Variation with Mach number of the base pressure coefficients for a wing-body configuration.

[redacted]

[redacted]

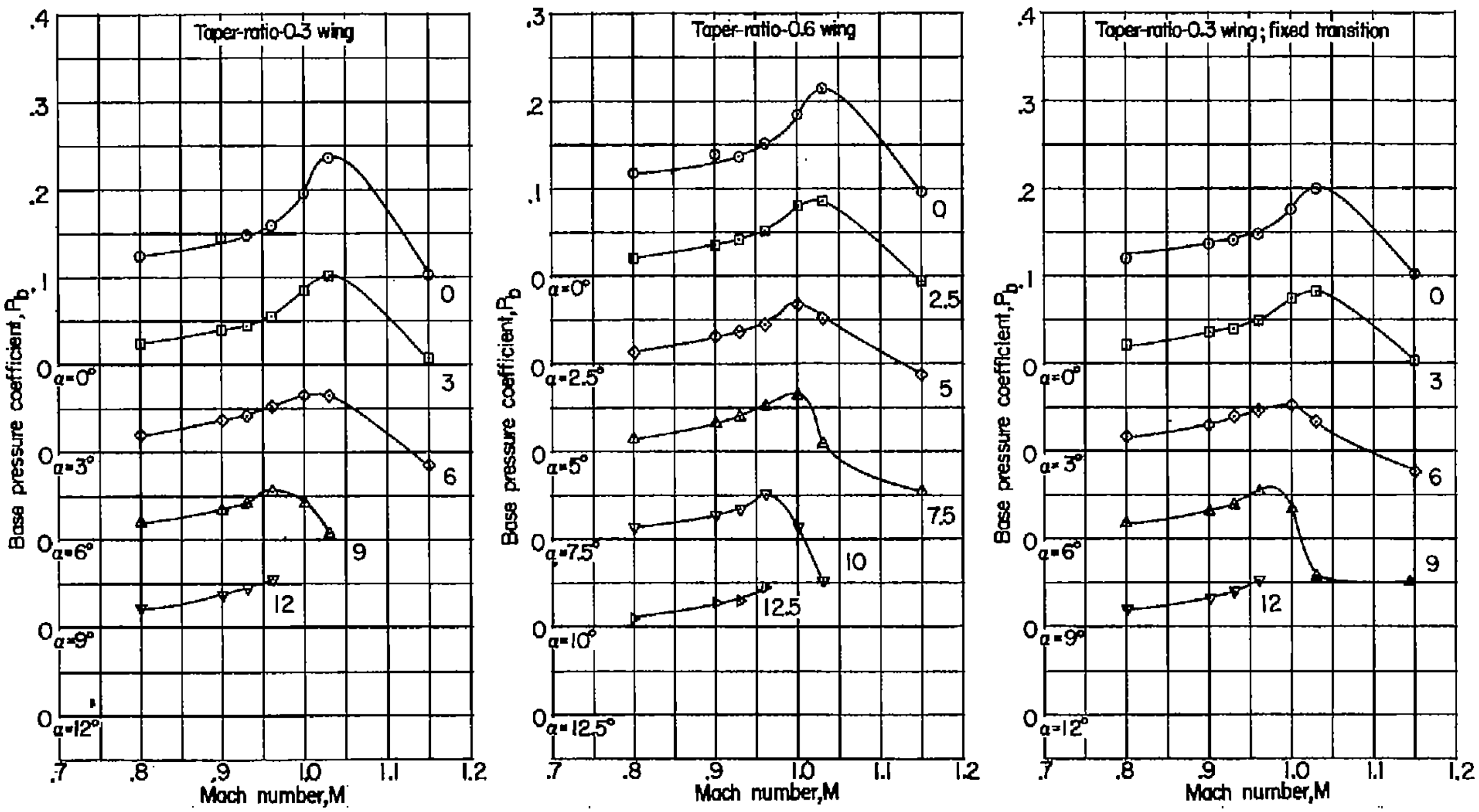

(b) Indented body.

Figure 6.- Concluded.

[redacted]

[redacted]

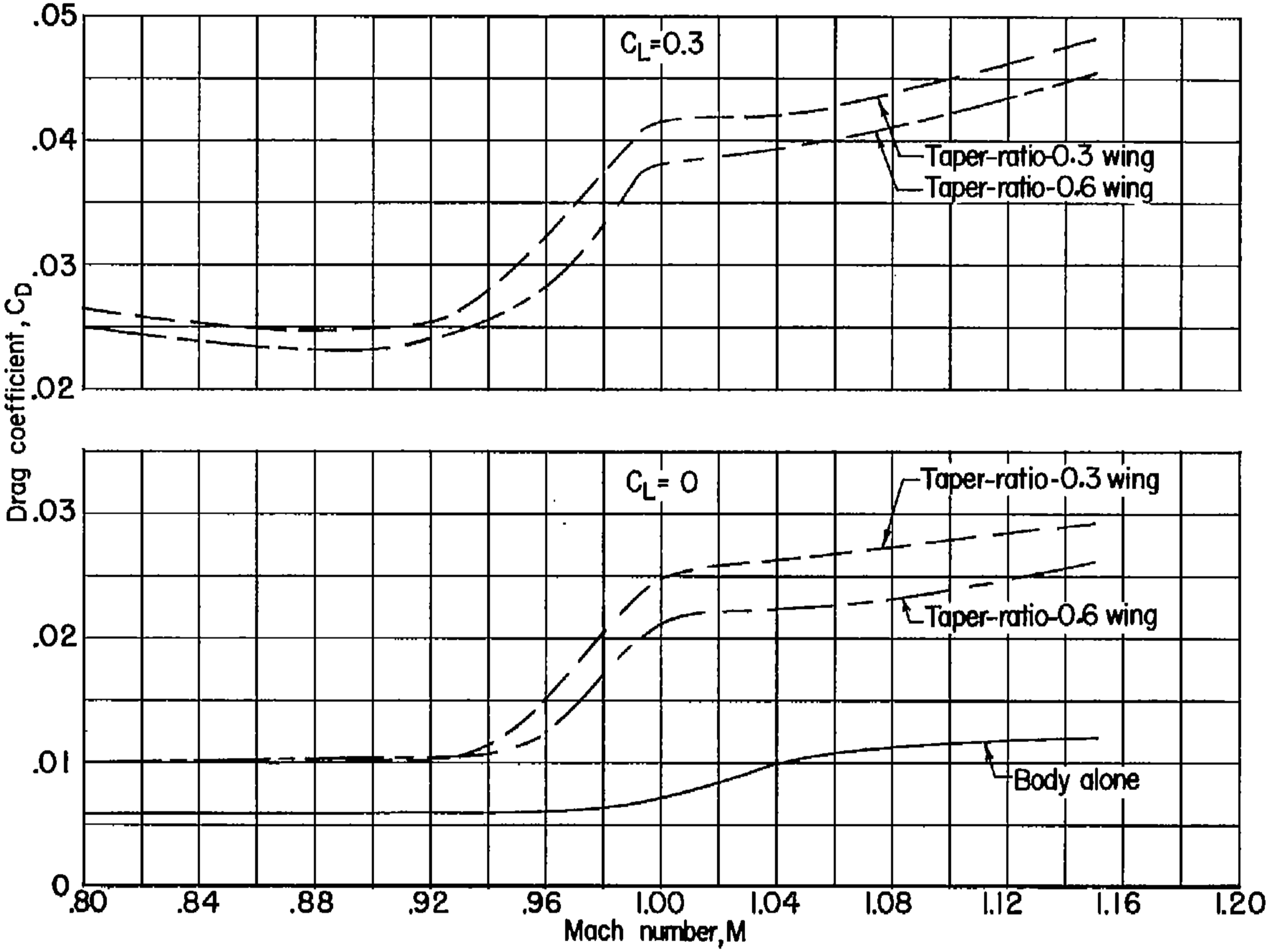

Figure 7.- Effect of taper ratio on the variation of drag coefficient with Mach number for lift coefficients of 0 and 0.3. Basic body.

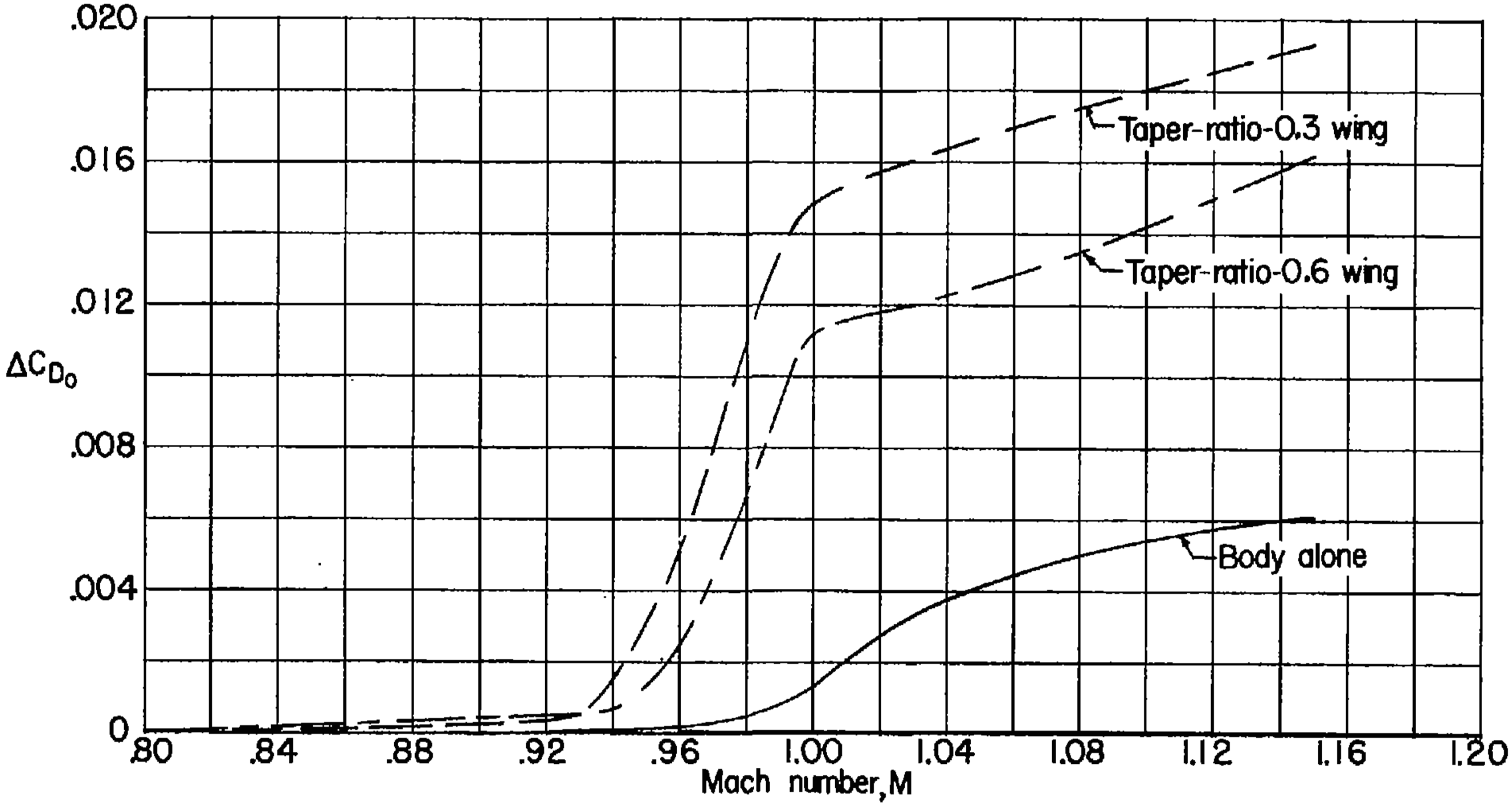

Figure 8.- Effect of taper ratio on the variation of drag-rise coefficient with Mach number. Basic body.

[redacted]

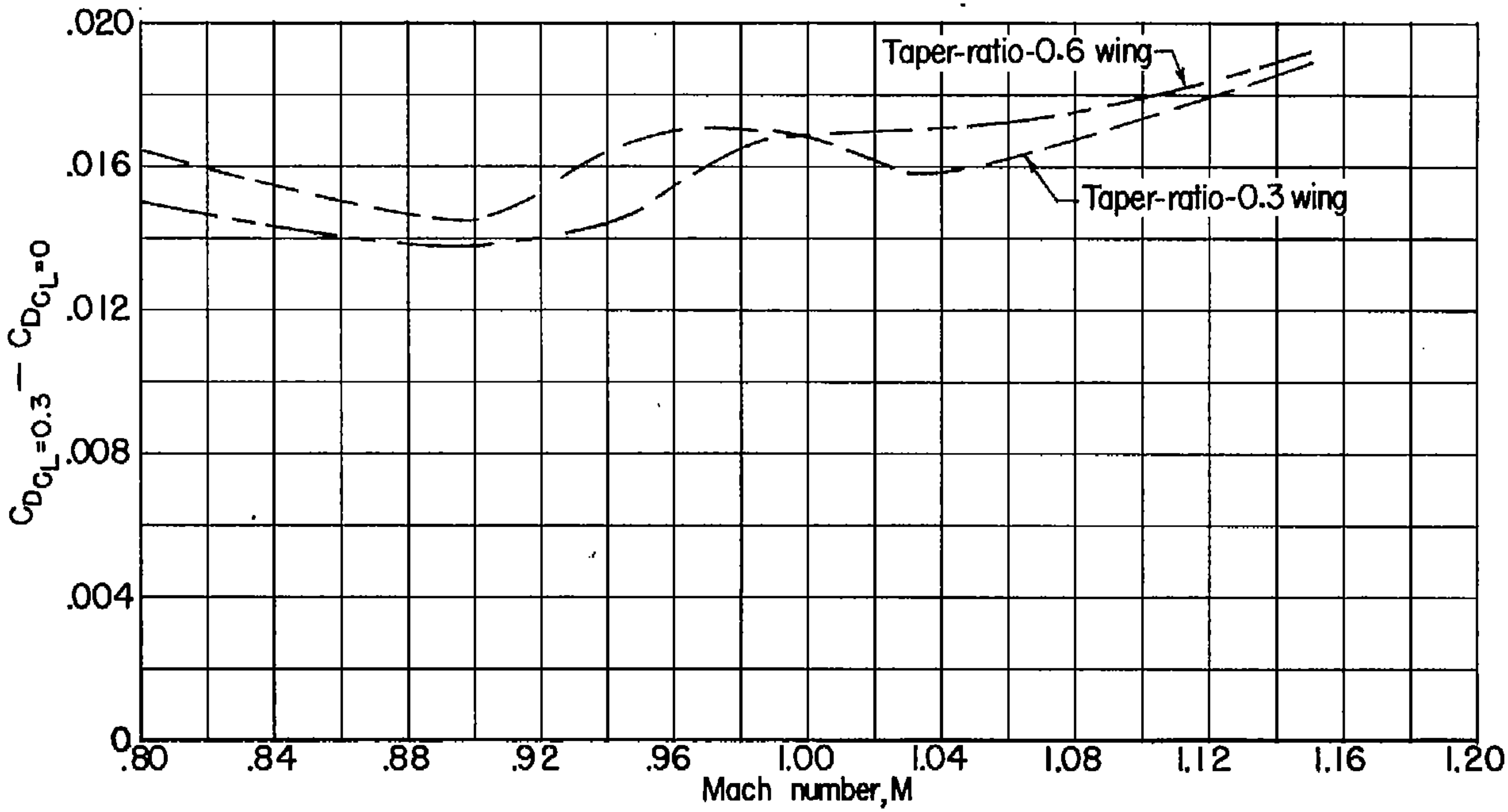

Figure 9.- Effect of taper ratio on the variation of incremental drag coefficient between lift coefficients of 0 and 0.3 with Mach number. Basic body.

[redacted]

[redacted]

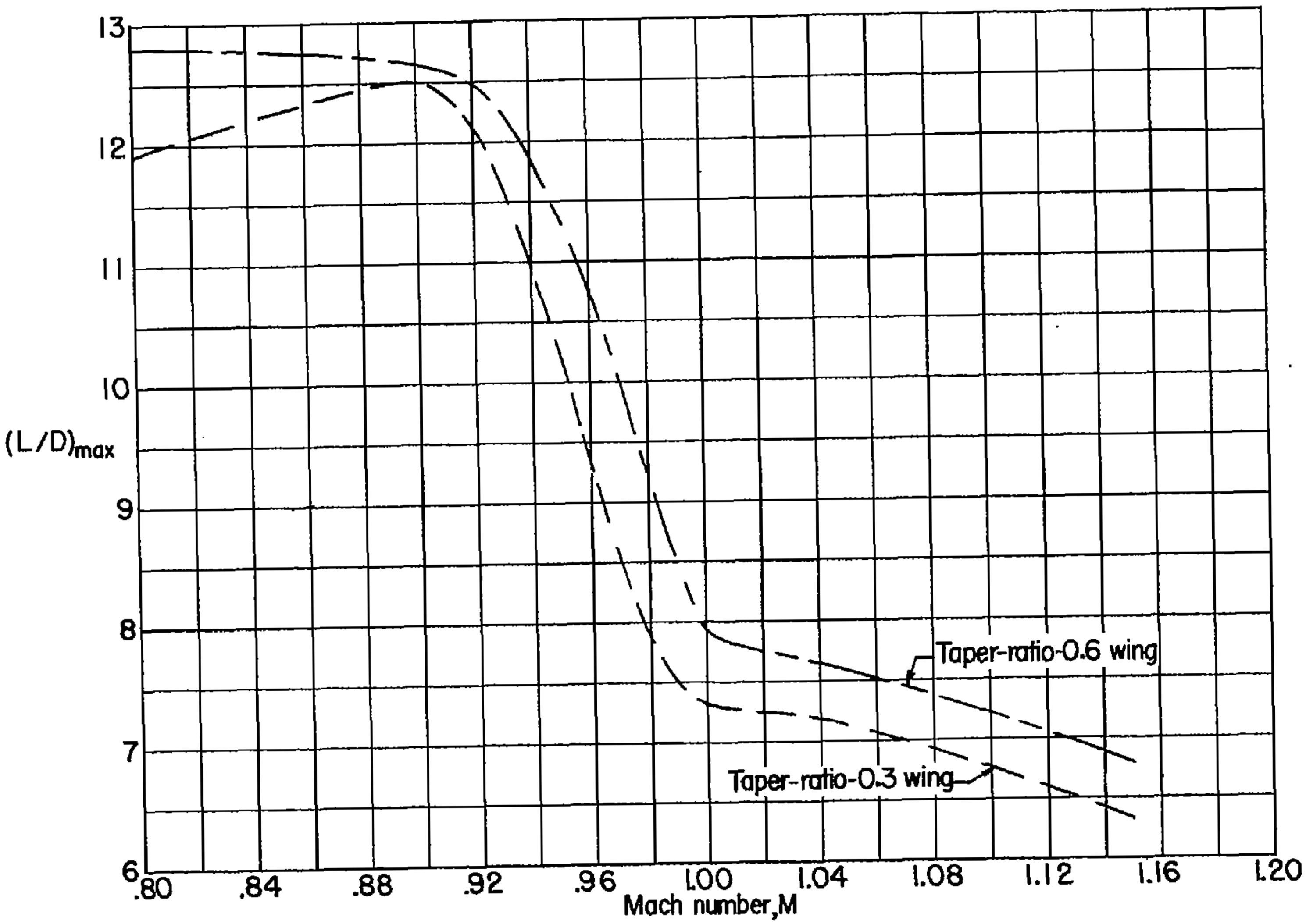

Figure 10.- Effect of taper ratio on the variation of maximum lift-drag ratio with Mach number. Basic body.

[redacted]

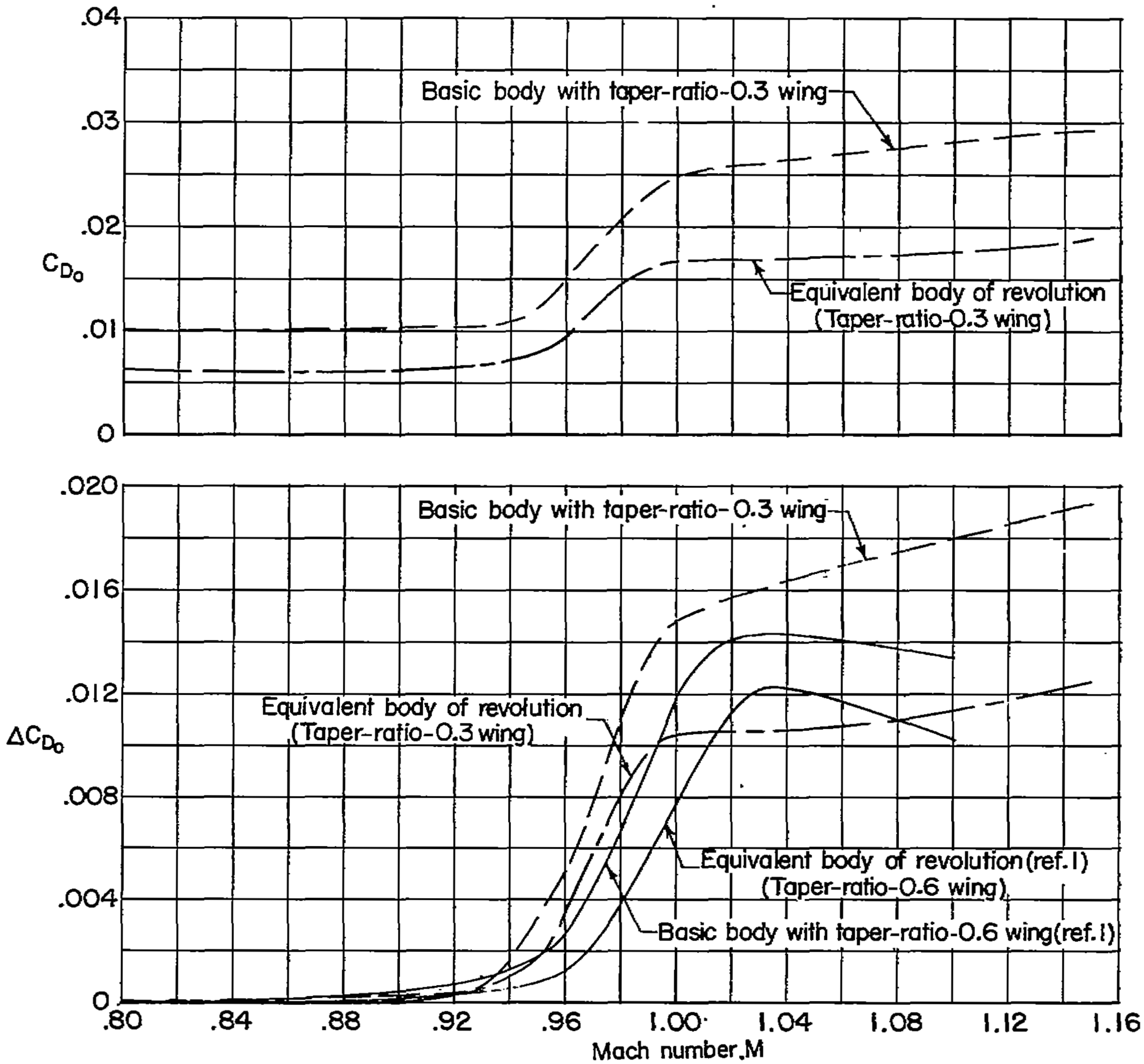

Figure 11.- Variation of zero-lift drag coefficient and drag-rise coefficient with Mach number for a wing-body configuration and a body of revolution simulating the same wing-body configuration.

[redacted]

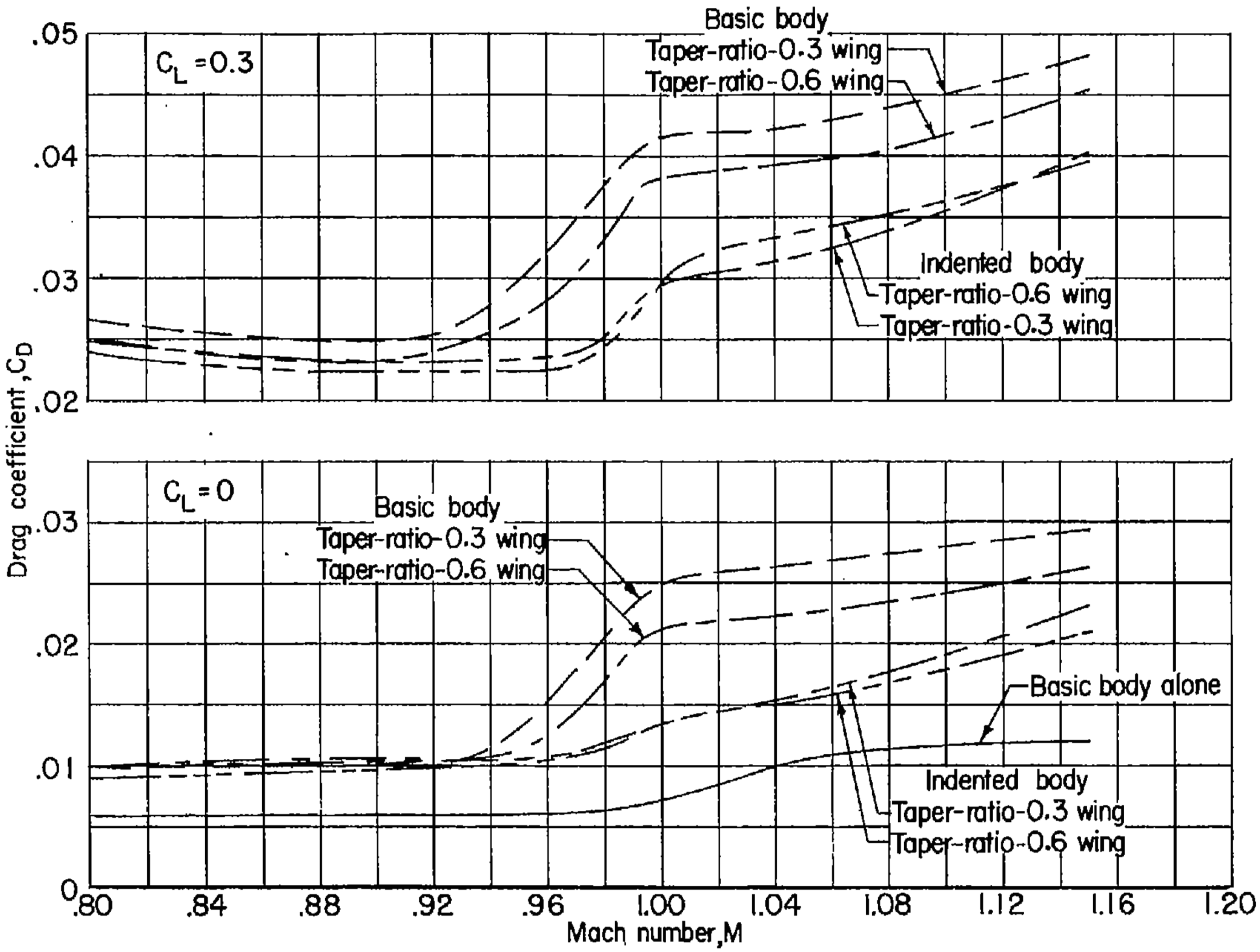

Figure 12.- Effect of body indentation on the variation of drag coefficient with Mach number for lift coefficients of 0 and 0.3 for two wings with different taper ratios.

[redacted]

[redacted]

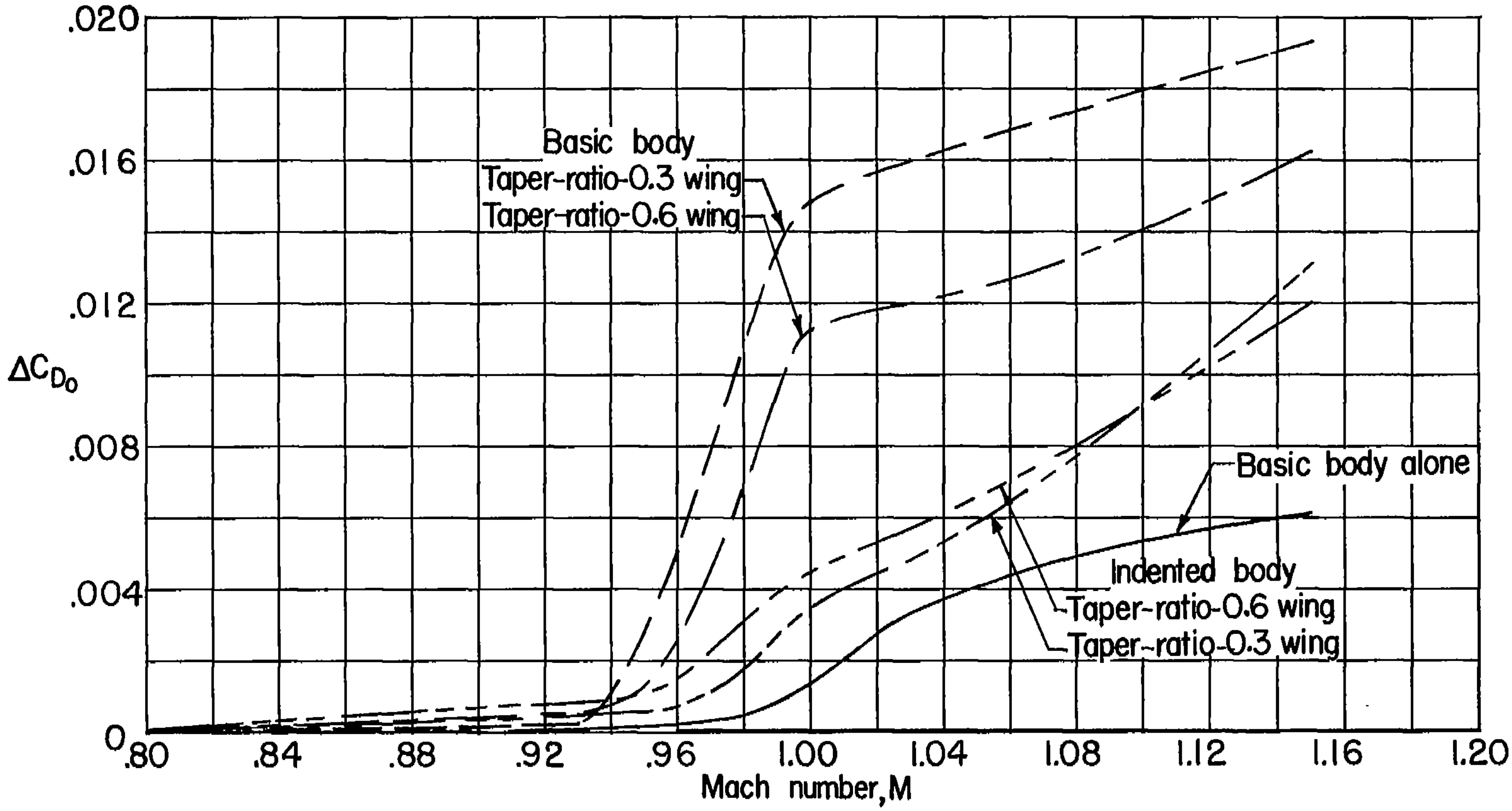

Figure 13.- Effect of body indentation on the variation of drag-rise coefficient with Mach number for two wings with different taper ratios.

[redacted]

[redacted]

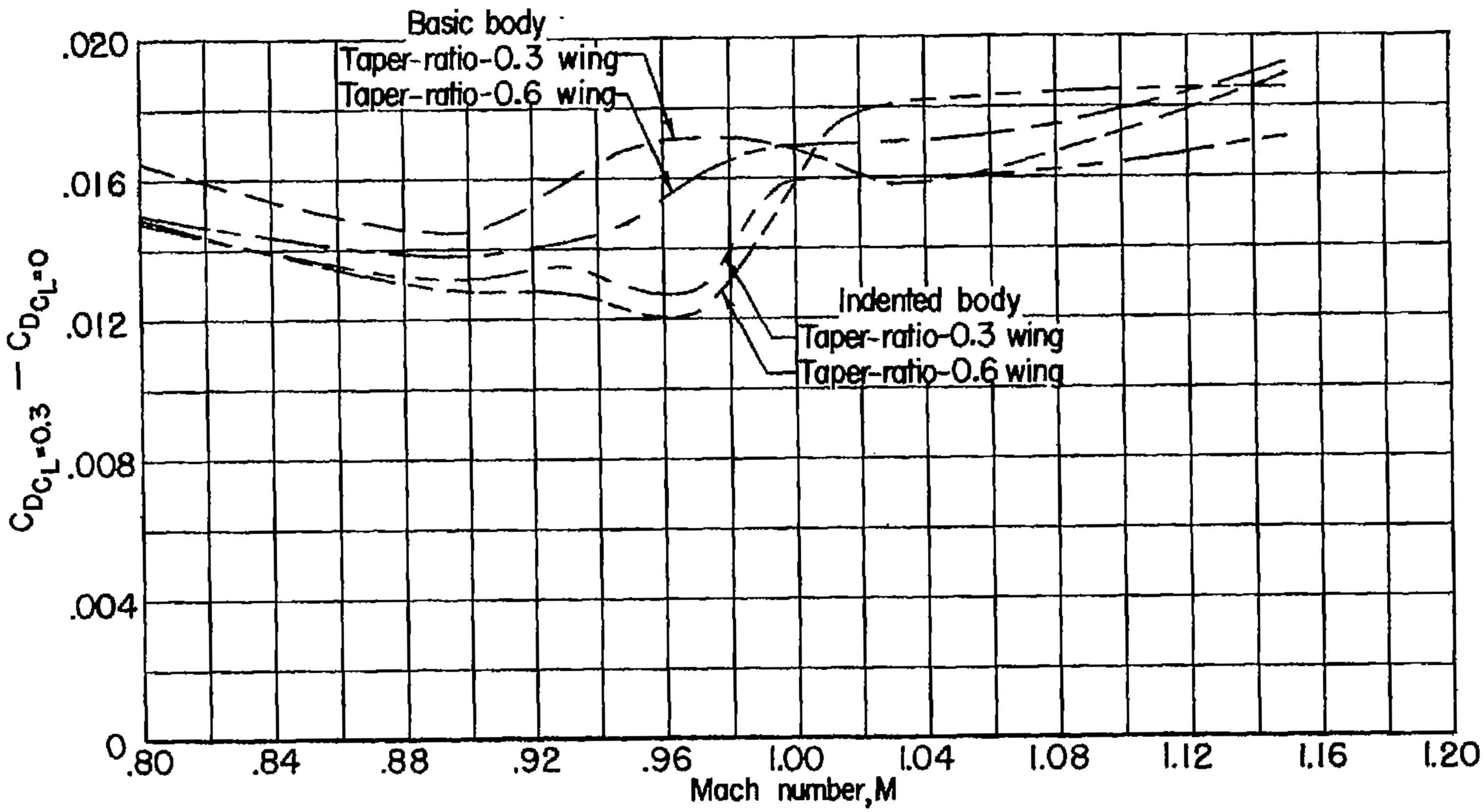

Figure 14.- Effect of body indentation on the variation of drag due to lift at a lift coefficient of 0.3 with Mach number for two wings with different taper ratios.

[redacted]

[redacted]

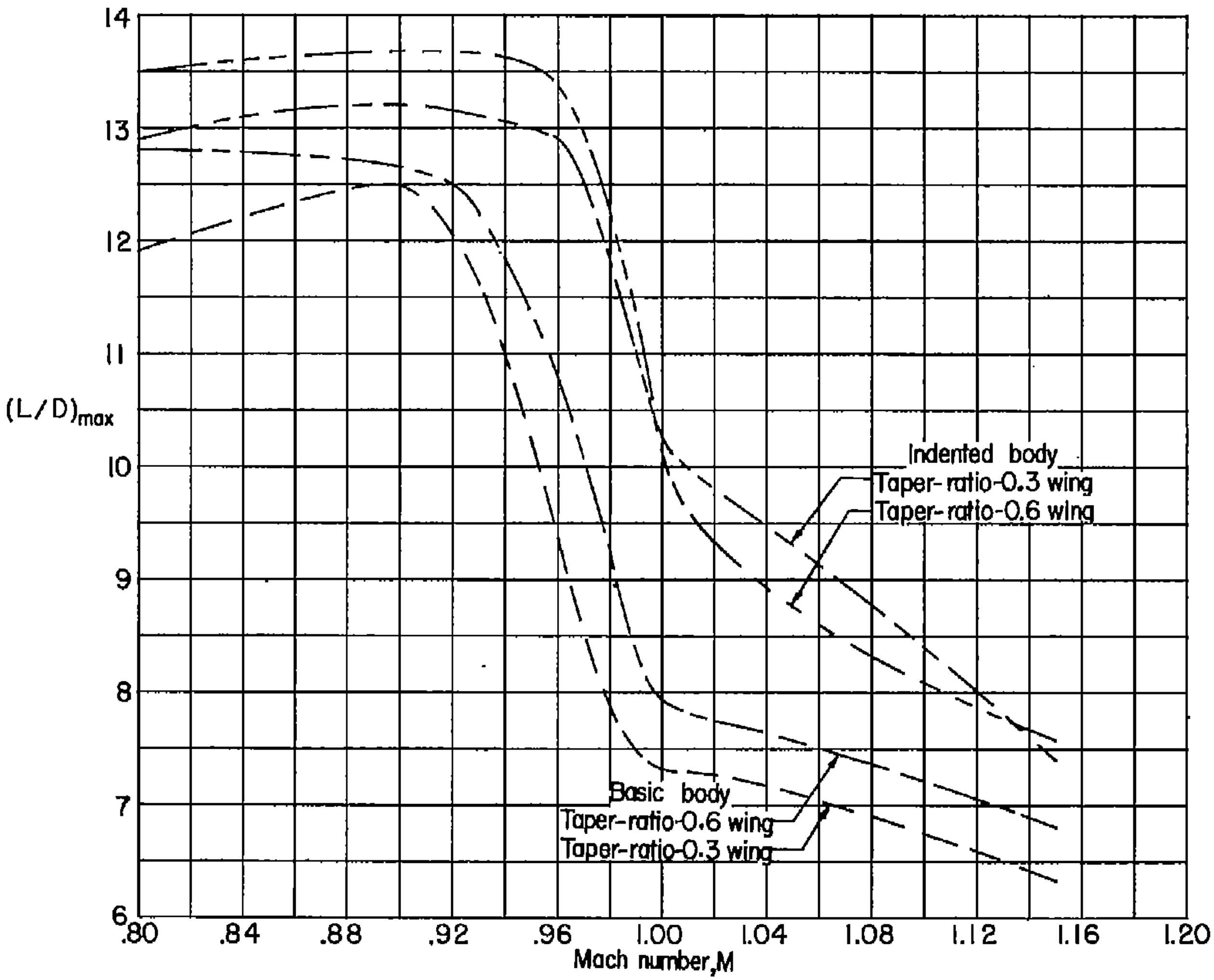

Figure 15.- Effect of body indentation on the variation of maximum lift-drag ratio with Mach number for two wings with different taper ratios.

[redacted]

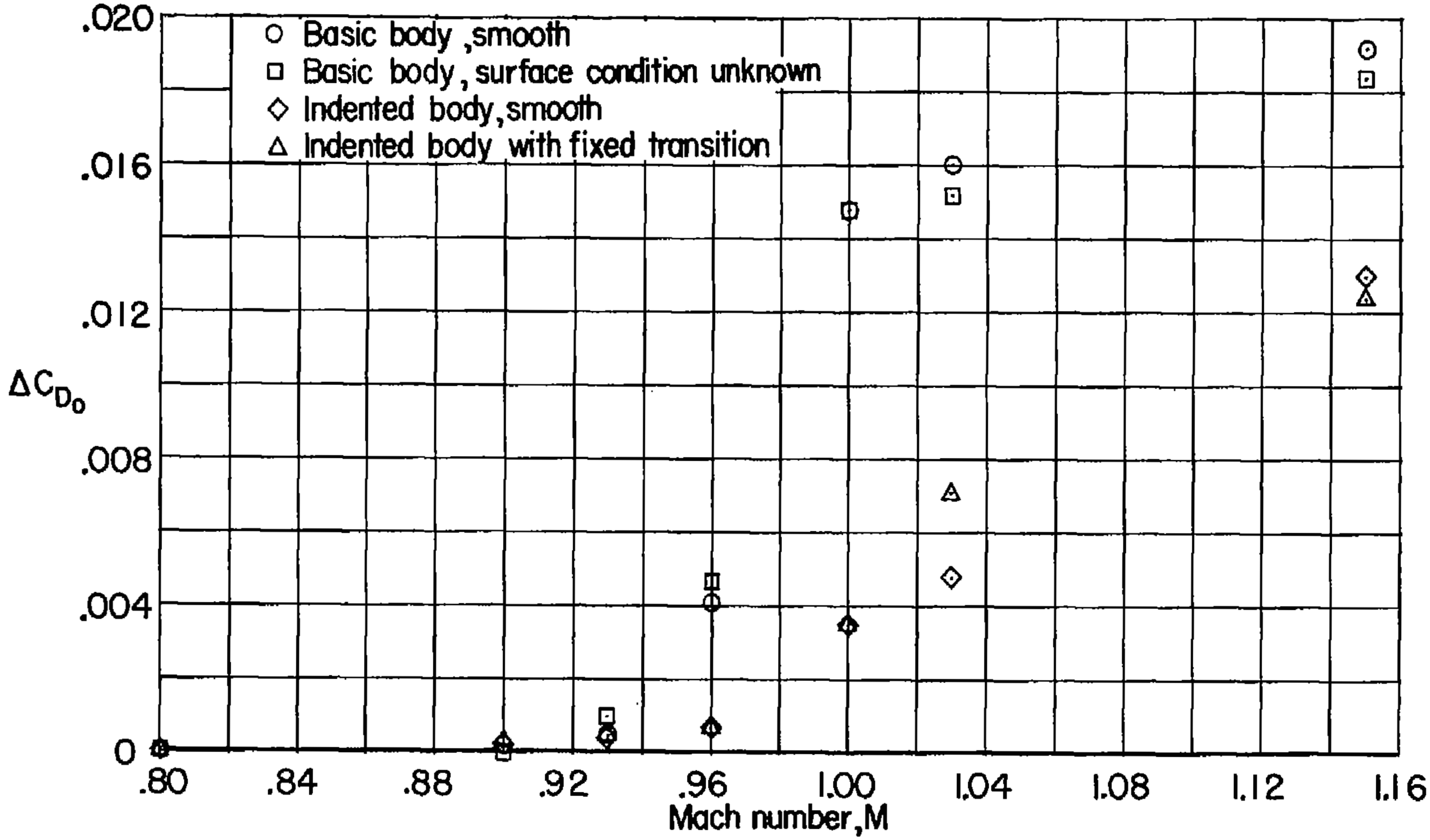

Figure 16.- Effect of fixed transition and uncontrolled surface roughness on the variation of drag-rise coefficient with Mach number for the 0.3-taper-ratio-wing—body configuration.

[redacted]

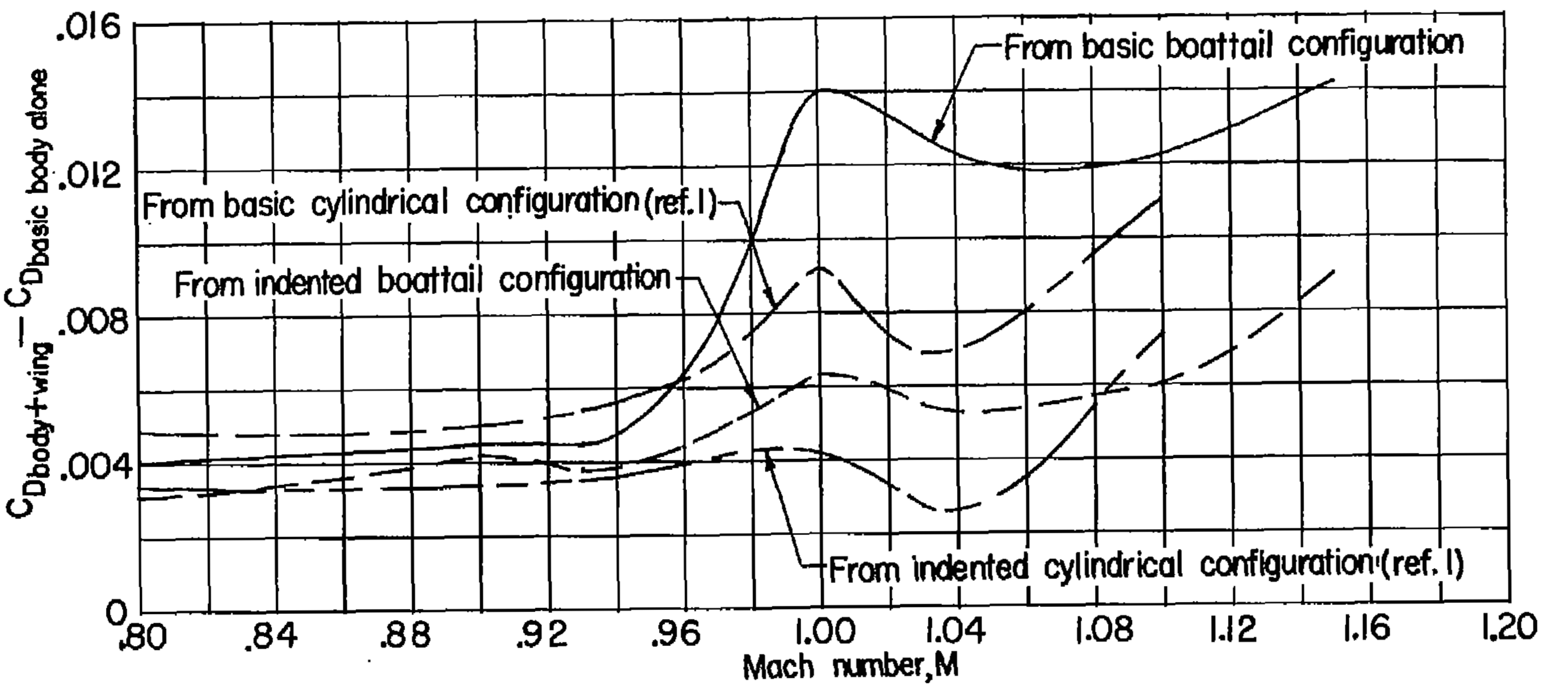

Figure 17.- Effect of body indentation on wing-body interference for the 0.6-taper-ratio-wing—body configurations.

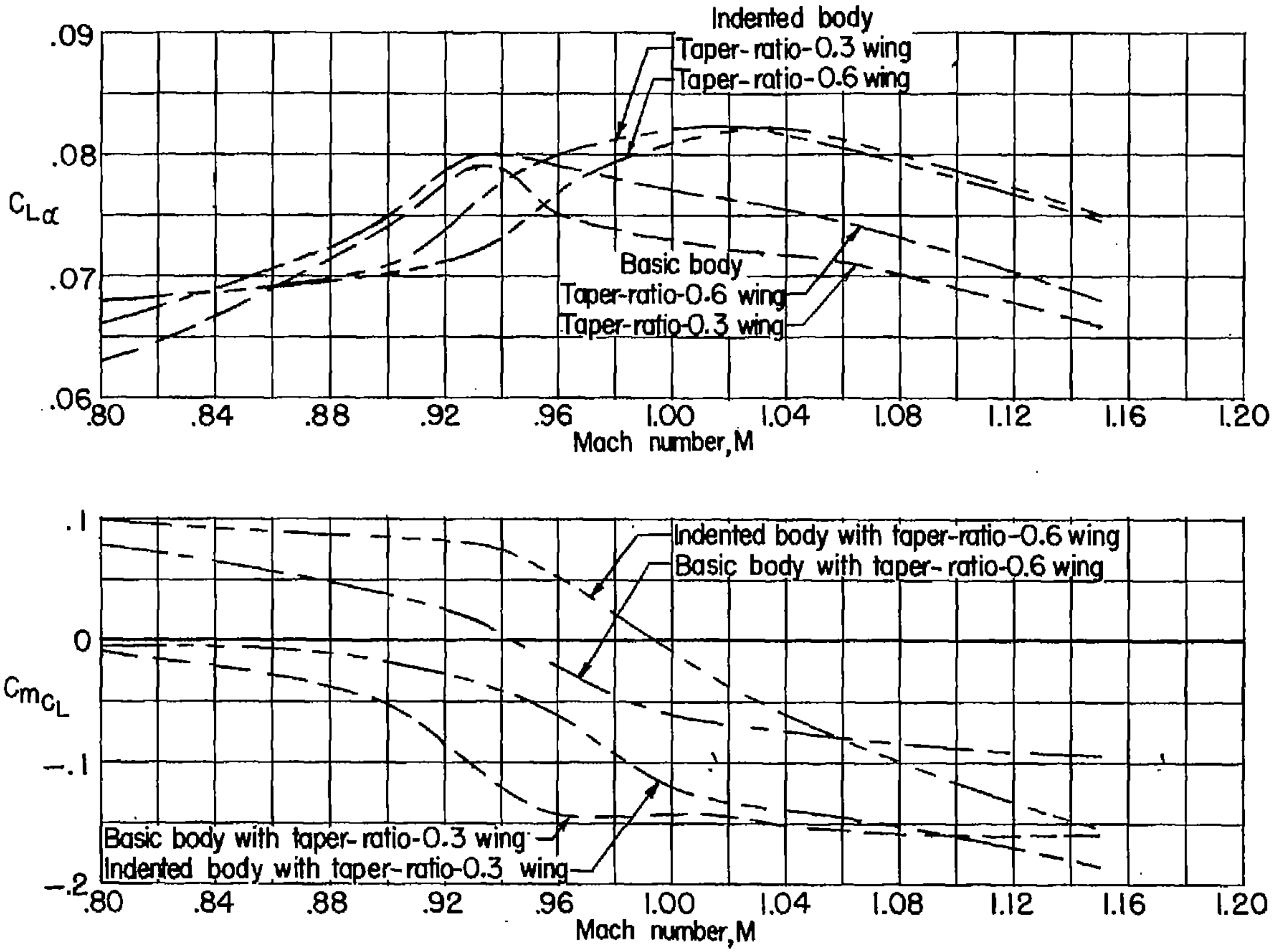

Figure 18.- Effect of taper ratio on the variation of lift-curve slope and the longitudinal stability parameter with Mach number.

[redacted]

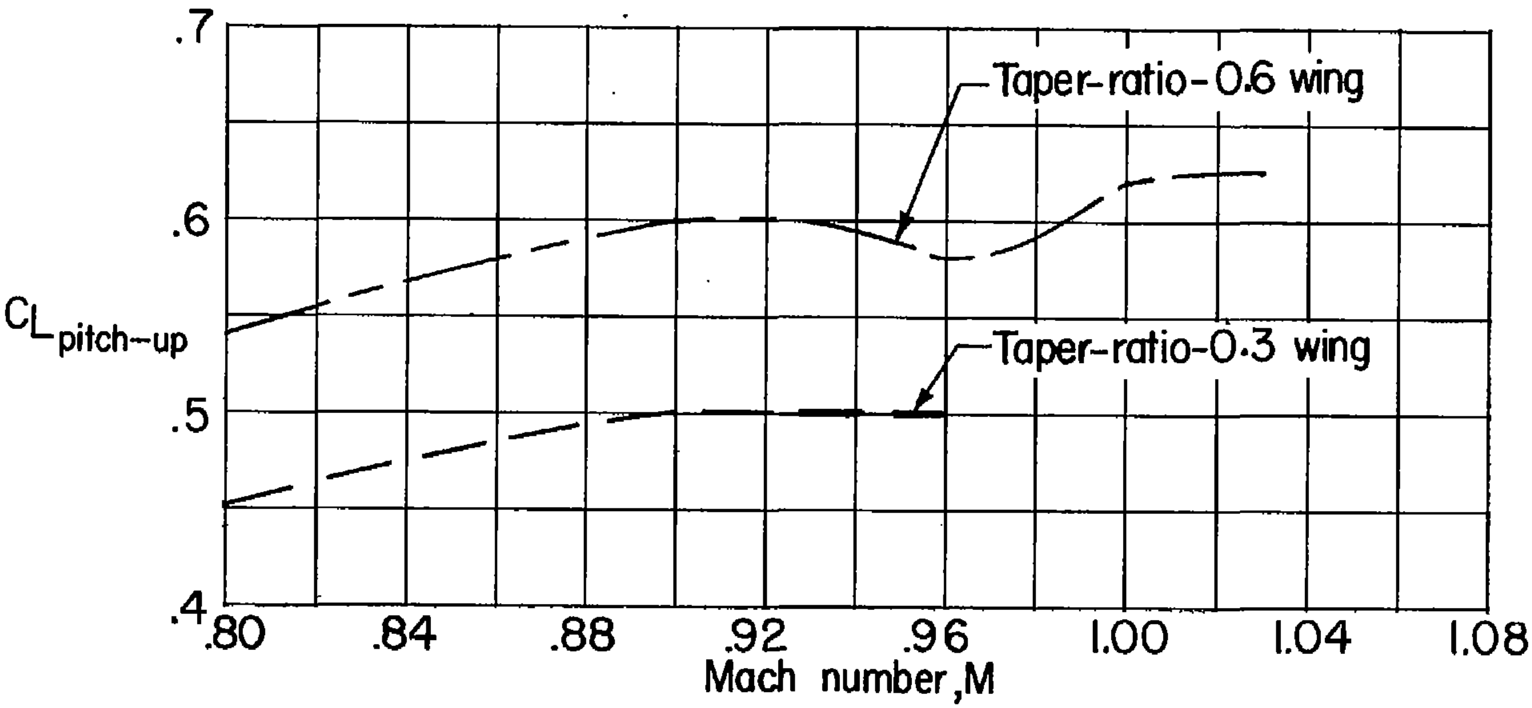

Figure 19.- Effect of taper ratio on the variation of lift coefficient for pitch-up with Mach number. Basic body.